Sustainable Cities and Society 115 (2024) 105834

Contents lists available at ScienceDirect

Sustainable Cities and Society

journal homepage: www.elsevier.com/locate/scs

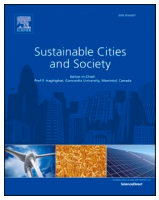

Smart feasibility optimization of hybrid renewable water supply systems by digital twin technologies: A multicriteria approach applied to isolated cities

Miguel Tavares [a], Modesto Pérez-Sánchez [b,*], Armando Carravetta [c], Oscar E. Coronado-Hernández [d], P. Amparo López-Jiménez [b], Helena M. Ramos [a]

[a] Civil Engineering, Architecture and Environment Department, CERIS, Instituto Superior Técnico, Universidade de Lisboa, 1049-001 Lisboa, Portugal
[b] Hydraulic and Environmental Engineering Department, Universitat Politècnica de València, 46022 Valencia, Spain
[c] Department of Hydraulic, Geotechnical and Environmental Engineering, Università di Napoli Federico II, 80125 Naples, Italy
[d] Instituto de Hidráulica y Saneamiento Ambiental, Universidad de Cartagena, Cartagena 130001, Colombia

ARTICLE INFO

Keywords:
Hybrid renewable systems
Digital twin technologies
Solver optimization algorithm
Multicriteria approach
Water Supply
Isolated Cities

ABSTRACT

This research presents a multicriteria approach for the best hybrid water supply solution of a multipurpose Pumped-Storage Hydropower (PSH) system, using the Generalized Reduced Gradient (GRG) method in Solver, with the optimization process considering key factors, such as Net Present Value (NPV), the number of energy conversion devices, renewable energy production, source availability, reservoir capacities, topographic constraints, and energy tariffs. The methodology combines a literature review, methodological development, and machine learning applications for hybrid water-energy systems. Results indicate that solar-only solutions are insufficient in high hydropower potential scenarios while integrating wind turbines significantly enhances energy production and profitability by generating surplus energy for grid sales. The timing of energy sales and the incorporation of battery storage also impact NPV, which can exceed 180 million euros. Wind energy contributes to continuous profitability and optimized system performance, particularly in isolated regions. The PSH system can manage 130,000 cubic meters of water daily, storing 25 MWh of energy, and reducing CO_2 emissions by over 18,000 tonnes per year. These findings highlight the importance of renewables, such as wind energy, and effective operational management. It enhances the economic viability and environmental sustainability of hybrid water-energy systems.

1. Introduction

Water is a valuable resource, that is necessary for many human activities as well as the life cycle (Moasheri et al., 2021). Rising demand and decreasing freshwater resources necessitate monitoring water consumption to manage growing stress (Kavya et al., 2023). To reduce the impact of these human factors, the application of artificial intelligence to water distribution systems is transforming them by enhancing their efficiency, sustainability, and resilience (Morosini et al., 2021). The use of these techniques combined with the management of big data analytics contributes to improving the feedback of the models to reduce errors in the water simulation models (Kamyab et al., 2023). These techniques not only lead to improved efficiency and resilience of the hydraulic systems through minimizing the pressure in the system (Magini et al., 2023), evaluation of distribution flows (Suresh et al., 2022), or reduction of leaks by using the pressure reduction valves (Bermúdez et al., 2022), or replacement of pipes, reaching increases of performance between 36 and 65% in the water distribution system, with the reduction of the run computational time (Jafari et al., 2023). Including optimization procedures of hybrid systems in wastewater treatment plants is crucial to improve their performance and reduce the carbon footprint in wastewater regeneration (Awad et al., 2023).

Previous references showed that advanced algorithms and machine learning techniques enable the optimization of water resource management, demand prediction, and early detection of water and energy losses or infrastructure failures. These predictive solutions facilitate real-time decision-making for water managers (Fu et al., 2022), improve the monitoring and control of complex networks (Wang et al., 2021), and allow for the creation of digital twins, that virtually replicate the system behavior (Wu et al., 2023), optimizing operations and maintenance. This leads to more efficient resource use, cost reduction, and improved environmental sustainability in water distribution systems (Xiang et al., 2021).

* Corresponding author.
E-mail addresses: mopesan1@upv.es (M. Pérez-Sánchez), ocoronado@utb.edu.co (O.E. Coronado-Hernández), hramos.ist@gmail.com (H.M. Ramos).

https://doi.org/10.1016/j.scs.2024.105834
Received 26 August 2024; Received in revised form 12 September 2024; Accepted 18 September 2024
Available online 21 September 2024

Symbology and Acronyms

α_P	Temperature Co-efficient of Power
C	Consumption
Cap	Capitation
CF	Cash Flow (€)
Cov	Covão
Δ_t	Time Interval (s)
E	Energy (kWh)
E_c	Energy Consumption (kWh)
f_h	Water Consumption Factor
f_p	Peak Factor
GPV	General Purpose Valve
G_T	Incident Sollar Irradiance (kW/m^2)
$G_{T,\ STC}$	Incident Sollar Irradiance at standard Test conditions (kW/m^2)
h	hour
$H_{downstream}$	Head of the Downstream Reservoir (m)
H_t	Pump Net Head (m)
H_u	Turbine Net Head (m)
$H_{upstream}$	Head of the Upstream Reservoir (m)
INV	Initial Investment (€)
J	Unit Head Loss (m/m)
l	Length (m)
N	Number of units
NPV	Net Present Value (€)
O&M	Operation and Maintenance Costs (€)
P	Power (kW)
p	pumping
PAT	Pump as Turbines
P_f	Proffit (€)
Pop	Population
P_{PV}	Power of the Solar PV (kW)
PVGIS	Photovoltaic Geographical Information System
Q	Flow Rate (m^3/s)
Q_c	Consumption Flow Rate (m^3/s)
Q_d	Distributed Flow Rate (m^3/s)
r	Discount Rate (%)
R	Reservoir
RE	Renewable Energies (Wind and Solar Power)
S	Supply
SG	Siemens Gamesa
Soc	Socorridos
SQ	Santa Quitéria
t	hydropower
T_c	Cell Temperature of Solar PV (°C)
$T_{c,\ STC}$	Cell Temperature Under Standard Test Conditions (°C)
u	Wind Velocity (m/s)
V	Volume (m^3)
V_s	Volume Stored (m^3)
Y_{PV}	Power Output During Standard Test Conditions (kWh)
γ	Specific Weight (N/m^3)
η	Efficiency (%)

Water management is linked to energy use, so distribution systems must address solutions that seek to achieve zero consumption while being self-sufficient in terms of water and energy (Ramos et al., 2022). Renewable energy resources applied to different technologies grew their applications in water distribution systems to innovate the search for environmentally friendly use of conventional energy resources (Sayed et al., 2023). The global energy crisis has driven many countries, particularly in Europe, to seek alternatives to imported fossil fuels, leading to global renewable capacity expansion (Hille, 2023).

The renewable energies advancements are mainly focusing on photovoltaic systems (PV), wind, and hydropower technologies (Khan et al., 2022). PV systems can be deployed in diverse settings from urban roofs to off-grid rural areas when the availability of solar radiation is enough (Mokhtara et al., 2021). The main disadvantage of solar systems is that they must be integrated with other clean generation systems that guarantee the continuity of energy generation, and absorb the surplus energy generated by the solar system (Ramos et al., 2024). Urban planning strategies that consider solar energy potential can further optimize the integration of PV technologies with other clean systems (Akrofi and Okitasari, 2022).

The use of wind energy systems has advanced significantly due to innovations in turbine design, aerodynamics, and materials. It enabled the increase of energy efficiency and capacity (Calautit and Johnstone, 2023). Wind power's versatility is evident in both onshore and offshore installations, each tailored to specific geographic conditions (Pérez-Collazo et al., 2015). The integration of energy storage solutions and smart grid technologies has addressed challenges, positioning wind power as a cost-effective source capable of meeting substantial global electricity demands (Khalid, 2024). The use of this technology increases the economic feasibility of remote area applications (Fathi Nassar and Yassin Alsadi, 2018)

By 2050, hydropower demand is projected to rise by 400 GW, utilizing ~64% of its potential and marking a 35% increase from current levels. Sustainable irrigation would require storing 460 km^3 of water annually, a 70% increase over today's storage (Schmitt and Rosa, 2024). Pumped-storage hydropower has also seen substantial growth, reaching 130 GW in 2021 in large systems. This scheme could be reproduced in micro pumped-storage in cities (Boroomandnia et al., 2024). The incorporation of these schemes in cities invites the managers of water distribution systems to establish the concept of smart cities using digital twin models to maximize the hydraulic efficiency of the systems, as well as the energy efficiency and integration of different clean energy solutions (Alonso, 2024). The levelized cost of electricity (LCOE) for utility-scale hydropower projects remains competitive, and lower than that of fossil-fuel-based projects (Xiang et al., 2024). The integration of the different renewable systems (PV, Wind, and pumped-storage hydropower-PHS) got LCOE values between 0.03-0.05 €/kWh (Ren et al., 2024). As example, PHS contributed around 15 % in covering the annual load energy (Nassar et al., 2021)

The energy transition to greener systems has become a key focus in climate policy agendas worldwide of different countries and cities (Karlilar Pata and Balcilar, 2024). Replacing fossil fuels with clean energy alternatives is crucial for achieving global climate-suited conditions and reaching different sustainable development goals (Garcia et al., 2024). This is crucial in the supply systems since the current urban drinking water systems are under great resilience and resource procurement pressures, with hydraulic performance and energy efficiency values that are unsustainable under climate change conditions (Beker and Kansal, 2024). GHG emission factors across different cities ranged from 32 to 70 kgGHG/MWh, with carbon payback between 4.5 and 12 months (Nassar et al., 2024). These renewable energy systems improve the energy and sustainable indexes when the topography of their location is favourable to integrate the PHS, reducing the LCOE values (Nassar et al., 2023).

This calls for developing intelligent methodologies that can be fed by databases and are based on artificial intelligence algorithms. These procedures can optimize the management of different energy systems (Alhasnawi et al., 2024). The main goal is to maximize the energy efficiency and the overall effectiveness of the system over a lifetime, considering the variation in terms of water demands, wind, and

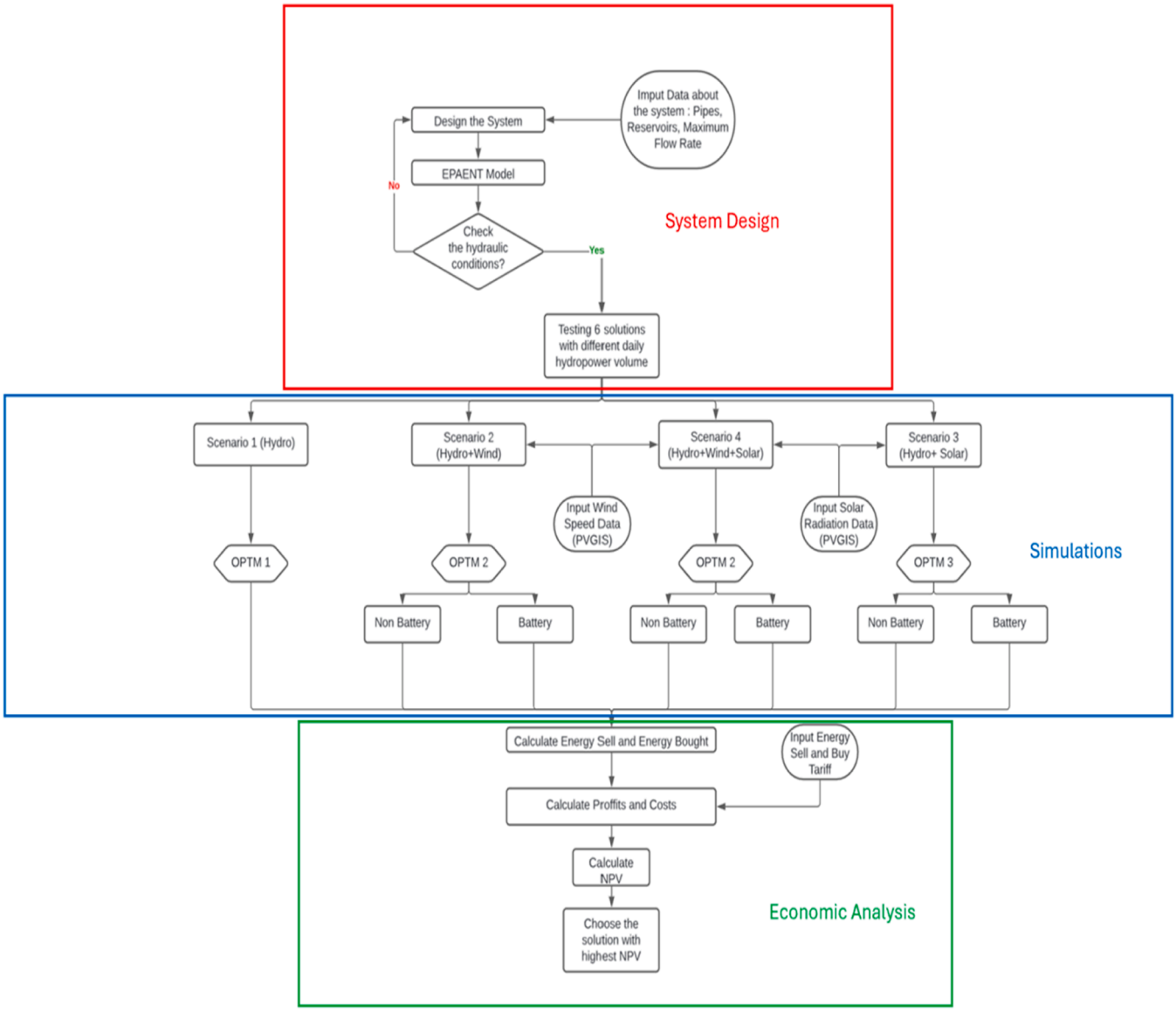

Fig. 1. Methodology

radiation, among others, reaching net-zero energy consumption (Elghaish et al., 2024). Incorporating renewable energy sources alongside grid power is recommended to reduce costs and potentially generate additional income (Nassar et al., 2024). This approach also decreases dependence on fossil fuels and contributes to mitigating global warming (Hafez et al., 2020).

Although different analysed studies for water supply systems, this research proposes a new multicriteria approach, which is based on an optimization algorithm created in Solver, with a single-objective function optimization of the Net Present Value (NPV) using the Non-Linear Generalized Reduced Gradient (GRG) method. It considers different criteria for attending to the system requirement in terms of sources availability, space to install them, the volume of water available in the upper and bottom reservoirs, energy tariffs, and all-time guaranteeing the water demand for the populations. The novelty of the optimization is to introduce not only the technical operation but also to consider the economic feasibility and environmental impact on real systems that are currently operating. This research work is structured as follows: Section 1, includes a detailed and recent literature review on the subject of water supply systems and new advances for the improvement of the system efficiency. Section 2 presents the methodology and materials developed in this research from different optimization stages and model development, presenting the case study, data collection, and lifetime analysis, with respective formulations and system definitions. Section 3 presents the machine learning for the hybrid solutions with the developed optimization algorithm and hydraulic system building model, and Section 4 enhances the model results and discussion for different system characteristics such as with only hydro, hydro with other renewables, including batteries or not, and develop a comparison between solutions. Section 5 states the main conclusions and limitations of this research work.

2. Methodology and materials

A new methodology for optimizing hybrid renewable water supply systems using digital twin technologies and a multicriteria approach was developed, focusing on isolated cities. This methodology presents a multicriteria approach for the best hybrid water supply solution of a multipurpose Pumped-Storage Hydropower (PSH) system, using the Generalized Reduced Gradient (GRG) method in Solver, with the optimization process considering diversified key factors. The novelty is the combination of different factors such as Net Present Value (NPV), the

number of energy conversion devices, renewable energy production, source availability, reservoir capacities, topographic constraints, and energy tariffs. as well as the limitations imposed by real system constraints. The optimization methodological proposal is divided into three stages. Besides, the programming algorithm comprises the operation in a real case study and the project design of renewable sources in terms of power and number of devices.

2.1. Optimization stages

This methodology allows the optimization process, from the system design stage, model simulations, to economic analysis (Fig. 1). Using the Excel Solver tool, a single-objective function optimization was performed utilizing the Non-Linear Generalized Reduced Gradient (GRG) method. This method includes the building of six solutions with different daily hydropower volumes, and four different scenarios with different combinations of renewable energy sources, which are optimized based on gradient patterns. The developed algorithm is dependent on the initial values of decision variables that often yield locally optimal solutions. To enhance the precision of the GRG method, the multistart option was enabled, combining GRG's computational efficiency with the complexity and accuracy of the Evolutionary method, which is based on genetic algorithms (GA). The population size was set to 200, with no predefined initial seed, and the convergence criterion remained at the Solver default value of 0.0001.

The design of the case study of the Socorridos Multipurpose System is the first step of this methodology. Initially, it provides data about the hydraulic circuit, the size of the three reservoirs, and the maximum flow rate for hydropower and pumping operations. With this data, it was designed the hydraulic circuit and the best respective characteristic curves of turbines and pumps. After developing the system, it was tested the hydraulic operation conditions in the digital twin hydraulic solver, and if the reply did not fulfill the system requirements and conditions, a new design was provided.

Six solutions with different daily hydropower volumes in Socorridos were tested. For each solution, four distinct scenarios were evaluated. The system with only hydro is called the normal operation, and the others include additional types of renewable energies to compensate for the pumping costs analyzed. To calculate the energy balance (i.e., sold and bought by the system), three types of optimizations were used depending on the new system configuration (i.e., Hydro+Wind, Hydro+Solar, Hydro+Wind+Solar), and it was also studied the influence of considering batteries in these scenarios.

Finally, knowing the energy balance considering the energy sold and the energy bought by the system, in each solution, the model allows the calculation of profits and costs, with the influence of sell and buy tariffs in this economic analysis. Adding to these values, the respective initial investment and the operation and maintenance costs, the NPV is estimated, and the solution with the highest NPV is then chosen.

This research was based on a real system and the complex model fits the limitations associated with the system characteristics, in terms of renewable energy sources availability and water demand for drinking and irrigation. The model only considers operational, economic, and environmental issues, but it does not consider the electric regulation and conversion components, as being outside of the scope of this research. However, an exhaustive evaluation was well-thought-out in the proposed methodology defined by (Nassar et al., 2022).

2.2. System components and formulations

2.2.1. Hydropower project

Hydropower projects offer a consistent energy source without releasing pollutants into the air. With a high flow rate, these systems can produce a substantial amount of daily energy, making them highly efficient.

However, the initial costs of these projects are substantial, and it's often not feasible to operate at a maximum flow rate daily, as maintaining a minimum water level in the upstream reservoir is necessary. To address this issue, some modern projects incorporate reversible operations, allowing water to be pumped during periods of low consumption and used for power generation during high demand (Beker and Kansal, 2024; Nassar et al., 2024, Nassar et al., 2023).

This approach enhances profitability. In hydropower projects, the turbine and pump net heads are the effective hydraulic energy that can be utilized for generating electricity and pumping a specific volume of water, respectively. These can be calculated using Eqs. (1) and (2).

$$H_u = H_{upstream} - H_{downstream} - Jl \tag{1}$$

$$H_t = H_{upstream} - H_{downstream} + Jl \tag{2}$$

The energy that a turbine can generate, and the energy needed to pump a certain amount of water depend on the flow rate and the net head. These values can be calculated using Eqs. (3) and (4).

$$E_{turbine} = \gamma Q H \eta_{turbine} \Delta_t \tag{3}$$

$$E_{pump} = \frac{\gamma Q H \Delta_t}{\eta_{pump}} \tag{4}$$

2.2.2. Reservoir volume

The water volume in the reservoir is calculated hourly, considering the turbine and pumped flow rates, the population's water consumption, and the existing water in the reservoir at each instant. Eqs. (5) and (6) represent the volume of water when the reservoir is in the upstream section of the gravity or pumped operation, respectively. It is crucial to determine this volume to ensure that the reservoir's capacity is not exceeded and that the volume never drops below zero at any given time.

$$V_{R\ h=i} = 3600\left(Q_{p\ h=i} - Q_{t\ h=i} + Q_{s\ h=i} - Q_{c\ h=i}\right) + V_{R\ h=i-1} \tag{5}$$

$$V_{R\ h=i} = 3600\left(Q_{t\ h=i} - Q_{p\ h=i} + Q_{s\ h=i} - Q_{c\ h=i}\right) + V_{R\ h=i-1} \tag{6}$$

If the reservoir is located downstream, when only the gravity operation occurs, the volume accumulated should be calculated using Eq. (7).

$$V_{R\ h=i} = 3600\left(Q_{t\ h=i} + Q_{s\ h=i} - Q_{c\ h=i}\right) + V_{R\ h=i-1} \tag{7}$$

2.2.3. Wind energy

Wind energy is another source of renewable energy that can be integrated into a hydropower project to offset the costs of pumping. It can generate substantial amounts of energy compared to solar panels and requires significantly less space for implantation. Although the initial investment in wind technology is high, it can become profitable in the long term if the conditions are favorable.

The energy generated by wind turbines is directly related to wind speed, which can be determined for a specific region and device height using an adaptation of the Prandtl law (Eq. (8)). While higher wind speeds result in greater energy production, it's important to consider that turbines can only operate within a specific range of wind speeds.

$$u(z) = u(z_R) \times \frac{ln\left(\frac{z}{z_0}\right)}{ln\left(\frac{z_R}{z_0}\right)} \tag{8}$$

In Eq. (8), Z_R is the height of the meteorological station in meters, Z is the hub height and Z_0 is the surface length in meters, which is 0,25 for a land with many trees and few buildings (Fluid Flow Friction 2024, Wind Turbine 2024, Saheb et al., 2014).

In this sense, the methodology can be supported by other formulations that allow the calculation of the wind power generated in the hybrid system, as defined by (Abdalla et al., 2023, Nassar et al., 2024), and proposing the shear coefficient in (Nassar et al., 2024).

2.2.4. Solar energy

Solar panels are extensively used today as they can convert solar radiation into electricity. They can be installed on rooftops, in greenhouses, gardens, and even deserts, where they operate with high efficiency. This equipment generates electricity only during daylight hours and can be particularly cost-effective in areas with low energy consumption. However, in locations with high energy demand, a significant amount of space is required to produce a substantial amount of electricity.

In solar panels, several factors affect the energy output, including solar irradiance and cell temperature. The energy produced by solar panels can be calculated using Eq. (9).

$$P_{PV} = Y_{PV} f_{PV} \left(\frac{G_T}{G_{T,STC}}\right) \left[1 + \alpha_P \left(T_c - T_{c,STC}\right)\right] \tag{9}$$

However, this solar-generated power can be estimated by using other formulations as defined by (Awad et al., 2022, Hafez et al., 2020). Besides, the cell temperature (T_c) is estimated using (Nassar and Salem, 2007).

Hence, with the integration of renewable energies, the energy available for sale from these devices is the difference between their energy production and the consumption by pump storage. This can be determined by applying Eq. (10).

$$E_{sold\ daily} = \sum_{i=1}^{24} E_{RE\ production} - E_{Consumption} \tag{10}$$

2.2.5. Batteries

The energy stored in a battery each hour is crucial for determining the appropriate battery size and ensuring its capacity is never exceeded. During off-peak periods, this storage can be calculated using Eq. (11).

$$E_{stored\ h=i} = E_{stored\ h=i-1} + E_{RE\ h=i} - E_{C\ h=i} \text{ If } i\langle 17 \text{ or i } \rangle 22 \tag{11}$$

Energy is sold to the grid for 6 hours during peak times when profits are highest. The amount of energy in the battery during these intervals is calculated using Eq. (12).

$$E_{stored\ h=i} = E_{stored\ h=i-1} + E_{RE\ h=i} - E_{C\ h=i} - \frac{E_{sold\ daily}}{6} \text{ If } If\ 17 \ll i \ll 22 \tag{12}$$

Mathematics formulation according to storage in batteries and inverter operation were defined by (Ahmed et al., Ahmed et al.).

2.2.6. Water consumption

When a hydropower project and pump storage system include a water supply component, it is crucial to determine the daily volume of hydropower and pumped to meet the population's water consumption needs.

The peak factor is used to calculate the maximum flow rate during periods of high demand, which is directly related to the population size in each region, as indicated in Eq. (13).

$$f_p = 2 + \frac{70}{\sqrt{Pop}} \tag{13}$$

Using the peak factor, the necessary maximum flow rate to meet daily water consumption needs can be determined (Eq. (14)).

$$Q_p = Pop \times Cap \times f_p \tag{14}$$

The volume of water that is used for water consumption varies from hour to hour and it can be determined using Eq. (15).

$$V_{hc} = \frac{f_h}{\sum_{h=1}^{24} f_h} \times Q_p \times 24 \times 3600 \tag{15}$$

2.3. System definition and configuration

The case study under analysis is located on Madeira Island (Fig. 2a). Its primary objectives are to supply water to the regions of Covão and Santa Quitéria and to generate electricity using two hydropower plants located in Socorridos and Santa Quitéria. Data on the populations of these two regions: Cova Region in which there are 42795 habitants, considering 3 habitants per house; (ii) Santa Quiteria Region in which there are 7089 habitants, considering 2.5 habitants per house. There are three reservoirs in each region, two hydropower plants, and one pump station, and the system operates reversibly. The scheme of the multipurpose Socorridos system is represented in Fig. 2b.

The water is collected from Levadas (top canals) and transported to Covão via an open channel with an annual flow rate of 300 l/s. A portion of the water reaching Covão is used for water supply, while the rest flows to Socorridos. There, some of the water is used to generate electricity at the Socorridos hydropower plant, with the remainder continuing to the Santa Quitéria hydropower plant for additional power generation. At Santa Quitéria, part of the water is allocated for water supply, while the rest is used for irrigation. The system is reversible, meaning that during certain periods, water is also pumped from the Socorridos reservoir to the Covão. Given that there is only one pipe connecting these two reservoirs, it is essential to ensure that the turbine periods do not overlap with the pumped periods. To control this situation, it is necessary to apply the developed optimization algorithm.

Various solutions are tested, incorporating solar panels and wind turbines to offset pumping costs and make the system carbon-free.

The system is composed of turbomachines (pumps and turbines), pipes, and reservoirs. Two pipes connect the three reservoirs in this system. The first pipe links Covão to Socorridos, and the second connects Socorridos to Santa Quitéria. Due to the large volumes of hydropower and daily pumped-water, these pipes have large diameters. Steel pipe, called C-S, connected the reservoirs Covão (Upstream reservoir) and Socorridos (downstream reservoir). It has a length of 1265 m and its diameter is 1,5 m. The other main steel pipe is called S-SQ. It has a length of 2000 m and a diameter equal to 0.56 m.

There are 3 groups of turbines and 4 groups of pumps operating in parallel at the Socorridos hydropower and pumping stations. In Santa Quitéria, the flow rate is significantly lower compared to Socorridos, resulting in the installation of only one turbine with a maximum flow rate of 1 m^3/s (Fig. 3).

The efficiency of the turbines and pumps is assumed to be 90% and 80%, respectively. The characteristics of these devices are detailed in Table 1.

The turbines and pumps operate in the Hydraulic Regulation Mode, and to determine the operating point, it is essential to know the system curves for both pumps and turbines. These curves can be calculated using Equations (1) and (2). Friction losses in the pipes depend on the

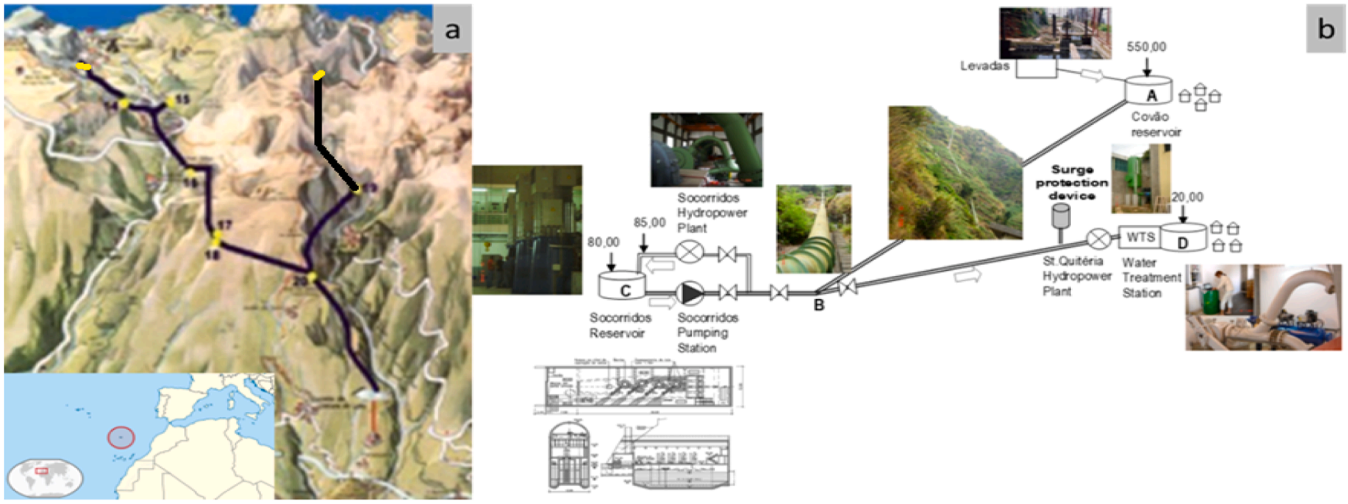

Fig. 2. Multi-purposes Socorridos System - Madeira Island: (a) topographic implantation; (b) system representation.

Hazen-Williams coefficient, which is 140 for unlined steel pipes (Fluid Flow Friction 2024). With these values, the pump and turbine system curves can be established and are presented in Table 2 and Fig. 4.

To standardise the system, the Covão and Socorridos reservoirs have been designed with the same capacity. However, the Santa Quitéria reservoir is smaller because the flow that reaches this region and the water supply necessities are lower. The characteristics of these three reservoirs are detailed in Table 3.

2.4. Data collection for the optimization procedure

This chapter presents data on wind speed and solar irradiance for the site selected for the renewable energy plant. This information is crucial for evaluating the energy potential of the area and determining the minimum number of devices required to offset the pumping costs. The data was provided by *PVGIS*, a tool developed by the *European Commission's Joint Research Centre (JRC)* (Kakoulaki et al., 2024).

2.4.1. Wind and solar data

Data from PVGIS was used to collect the average wind speed at a height of 10 m, recorded hourly over 15 years (2005-2020). Wind speed values for December 2007, 2014, and 2017 were excluded from the dataset due to being significantly higher than the average, potentially indicating extremely isolated meteorological events.

The wind turbine SG 2.1 -114, will have a rotor diameter equal to 114m, and a nominal power of 2.1 MW. The tower has a height of 153 m, and the turbine belongs to the Wind Class II. The power curve of the turbine is represented in Fig. 5a.

Considering the wind speed measurements at 10 m height, and using Eq. (5), it is possible to calculate the wind speed at the rotor. Wind speeds are typically higher during the winter months and lower in the summer. Additionally, wind speeds tend to be greater during daylight hours and lower at night, as illustrated in Fig. 5b.

Several types of solar panels were evaluated, and the model with the highest power peak was selected. The chosen device is the TopBiHiKu7 from Canadian Solar, which features bifacial technology and has 787 Wp (PARTNER 2024). The panels are mounted in a fixed position and are composed of crystalline silicon. Each device has an approximate efficiency of 23%, and a system loss of 14% was assumed, as this is the default value established by PVGIS. The slope and azimuth were optimized to 29° and 14°, respectively, with all panels oriented south. Based on these characteristics, hourly data on incident solar radiation was collected over 20 years (2005-2020) (Fig. 5c). The solar radiation database used is PVGIS-SAARAH2. Applying Eq. (9) and the provided data, it is possible to calculate the hourly energy production. Energy output tends to be higher in the summer months and lower in the winter. During daylight hours, production reaches its peak near midday.

2.4.2. Water consumption

Water consumption occurs in two populations: Covão and Santa Quitéria. For Covão, the consumption rate is 200 l/inh/day, while for Santa Quitéria it is 180 l/inh/day. Generally, the water consumption is higher close to lunch and dinner times, and lower during the afternoon and at night. Fig. 6 shows the daily water consumption volume for Covão (Fig. 6a) and Santa Quitéria (Fig. 6b), respectively.

2.4.3. Energy tariff

Electric tariffs denote the unit monetary value for selling and purchasing energy from the grid. These rates differ by region and season. Fig. 7, displays the buy and sell tariffs, respectively, for Madeira Island in 2023. It was considered that the winter months are January, February, March, October, November, and December. The remaining months belong to what is called the summer season.

Upon analyzing these two graphs, it can be concluded that the peak periods for energy buying and selling occur in the evening when consumption is at its highest, while the lowest values are reached at night, corresponding to decreased consumption. Additionally, the energy-selling tariff is generally lower than the energy-buying tariff, which suggests that optimizations are required to identify the optimal times for turbine operation and water pumping to ensure the economic viability of the hydropower system.

With regard to water consumption, tariffs fluctuate based on factors such as the type of usage, the region of consumption, household size, and the season. Covão and Santa Quitéria are residential areas within the same commercial unit, Câmara de Lobos. However, the average household size is larger in Covão (as indicated in Table 4), leading to higher water consumption per household, and thus, higher tariffs in this region. The tariffs for these two populations are summarized in Table 4. In this case, the summer tariff is applicable only during July, August, and September.

2.5. Lifetime analysis

For this research, an economic analysis, to find out the most cost-effective solution is developed. A lifetime analysis spanning 20 years was considered, focusing only on the equipment that would need replacement in the future. Given the anticipated fluctuations in prices over the coming years, two separate economic analyses were performed: one for 2025 and another for 2030. The cash flow can be calculated using Eq. (16).

$$CF = P_i - C_i \quad (16)$$

Profits (Pi) include revenues from energy sales to the grid, the benefits from water consumption, and subsidies for renewable energy set by the Portuguese Government. Conversely, costs (Ci) encompass the operation and maintenance of materials and devices, as well as expenses related to energy purchases.

The Net Present Value (NPV) is a key parameter in economic analysis that assesses the profitability of an investment. It can be determined by applying Eq. (17).

$$NPV = \frac{(CF)}{(1+r)^n} - INV \quad (17)$$

In this equation, the initial investment includes the initial cost of materials and devices, while the discount rate accounts for the present value of future cash flows, varying according to the type of business.

In some scenarios, the energy used in the pump operation comes from the grid, because renewable sources (wind and solar), cannot provide sufficient energy to satisfy the demand. This energy is associated with $C0_2$ emissions into the atmosphere, which are taxed in many countries of the European Union. This cost can be calculated using Eq. (18) (Mercedes Garcia et al., 2022).

$$E_{CO2} = G_{Energy} \times CO2_{factor} \times Emissions_{tax} \quad (18)$$

The Grid Energy (G_{Energy}), is the energy consumption to the grid, the CO2 factor is the mass of carbon dioxide emitted into the atmosphere per unit value of energy (0,331 kgCO2/kWh) and finally, the emissions tax is the tariff defined by the local authorities to penalize the emissions (0,1162€/kgCO2).

2.5.1. Materials and devices of hydropower and pump storage project

Pipes, turbines, and pumps are the only devices that were taken into account, for the initial investment and operation and maintenance costs of the hydropower and pump-storage project.

The annual operation (Fig. 8) and maintenance costs of civil works (pipes) and electromechanical equipment (turbines and pumps) represent 1% and 2% of the initial investment.

For pipes, the CAPEX was determined using specific equations for steel pipes (COST BASE 2024). An interpolation was made to determine the unit cost and it is assumed that its cost would remain constant in the future.

Electromechanical equipment represents the highest cost in a hydropower and pump-storage project. The Socorridos turbine CAPEX was estimated using the curves for Pelton turbines (Nassar et al., 2022). The initial cost of the Santa Quitéria turbine was calculated using Eq. (19), which is appropriate for Pelton turbines with a power range below 2 MW (Ogayar and Vidal, 2009).

$$C_{Pelton}(€/kW) = 17693 \times P^{-0,3644725} \times H^{-0,281735} \quad (19)$$

The CAPEX of the Socorridos pump can be determined using Eq. (20).

$$C_{PAT}(€/kW) = 150 + 2084P^{-1} \quad (20)$$

Operation and maintenance total costs and the respective investment, for civil works and electromechanical equipment are represented in Table 5 (Ramos, 2000). In this case, it was considered a discount rate of 5% in 2025 and 2030 (Seme et al., 2018).

2.5.2. Wind turbines, PV systems, and batteries

Wind turbines are notably expensive, with their capital expenditure (CAPEX) determined by their wind class (Satymov et al., 2022). For the selected device, the operation and maintenance costs are 21.2 €/kW/year in 2025 and 20 €/kW/year in 2030. The CAPEX for these turbines is 1228 €/kW in 2025 and 1161 €/kW in 2030. Using the specifications of SG 2.1-114 (Onshore 2024), the total O&M costs and the initial investment per unit turbine are detailed in Table 6. For wind projects, the discount rate is approximately 6.23 % in 2025 and 6.0 % in 2030 (Positioning 2024).

Solar panels are cheaper, and the costs are determined based on their power peak. The operation and maintenance costs for a single solar panel are 7.3 €/kWp/Year in 2025 and 0.28 €/kWp/Year in 2030, while the CAPEX is 0.33 €/Wp in 2025 and 0.28 €/Wp in 2030 (Vartiainen et al., 2020). The total O&M costs and the initial investment for the model described are shown in Table 6. For solar panels, it was considered a discount rate equal to 3.50 % in 2025 and 3% in 2030.

Batteries can have different sizes, based on the energy necessities, and they are more expensive when the storage capacity increases. Their costs would decrease very fast in the next few years, due to the energy transition. The CAPEX is 82,3 €/kWh and 33.54 €/kWh, for 2025 and 2030, respectively (EV Battery 2024). The operation and maintenance costs represent 1.5% of the initial costs.

3. Machine learning towards hybridisation

3.1. Solver optimizations

The Socorridos multi-purpose system is very complex, and during its operation, it must comply with certain restrictions relating to the maximum flow rate in the pipes, and the minimum and maximum levels of the reservoirs, and ensure that water distribution to the population is never affected. On the other hand, any solution should be as cost-effective as possible and, in some cases, reduce carbon emissions into the atmosphere.

Solver is an optimization tool for solving complex mathematical problems and was used to build the model. To run the simulations, it is necessary to define an objective function, and variable cells, add some constraints, and select the solving method. The GRG nonlinear with auxiliary evolution algorithm was chosen due to the non-linearity of these problems.

In the ***first scenario*** of optimisation, the goal is to maximise the Net Present Value (NPV). This optimisation is only applied to solutions that do not incorporate additional renewable energies and batteries. The variable cells involved in this process include the pumped and hydropower flow rates between Covão and Socorridos, as well as the hydropower (or gravity) flow rates between Covão and Santa Quitéria.

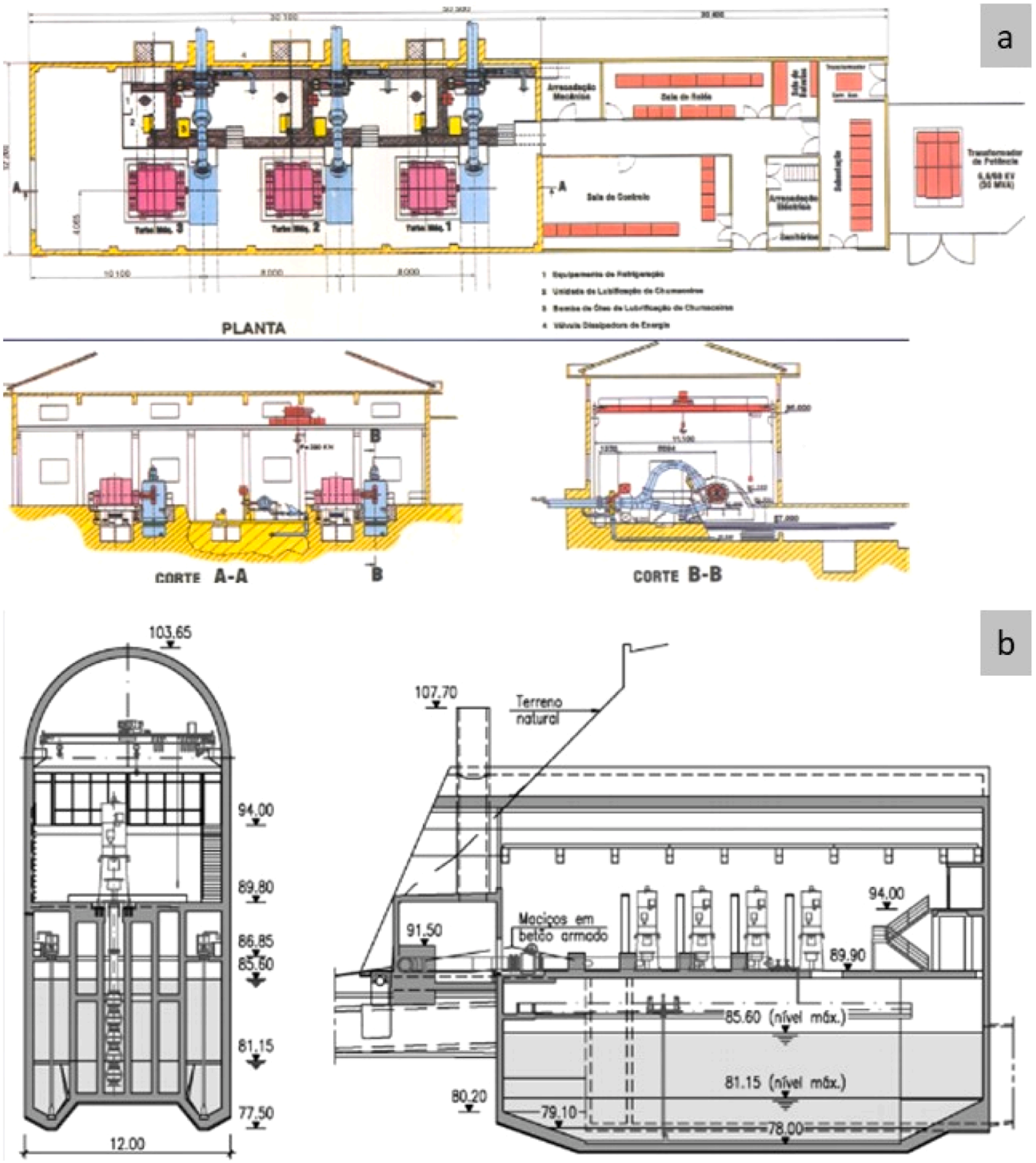

Fig. 3. Socorridos system: (a) Hydropower and (b) Pumping Stations.

Table 1
Characteristics of the hydraulic turbomachines.

Device	Location	Type	n° of groups	Displacement	Flow rate p/ group (m^3/s)	Maximum flow rate (m^3/s)
Turbine	Socorridos	Pelton	3	parallel	2	6
	Santa Quitéria	Pelton	1	-	1	1
Pump	Socorridos	PAT	4	parallel	0.7	2.8

Table 2
System curves in turbine and pump modes

Pipe	Operation mode	System curve [H (m); Q (m^3/s)]
Covão-Socorridos	Turbine	$Hu = 463,846 - 0,0314Q^{1.852}$
	Pump	$Ht = 470,00 + 0,19895Q^{1.852}$
Socorridos-Santa Quitéria	Turbine	$Hu = 223,751 - 38,1479Q^{1.852}$

Some restrictions were necessary to run the simulations and to find the maximum NPV, for each solution, which are presented as follow:

1) The flow rates for both turbine and pumping operations at Socorridos, as well as the hydropower flow rate at Santa Quitéria, must not exceed their respective maximum values. Above these values, the electromechanical equipment, turbines, and pumps, cannot work.

$$\begin{aligned} Q_{tS_{h=i}} &\leq 6\ m^3/s \\ Q_{pS_{h=i}} &\leq 6\ m^3/s \\ Q_{tSQ_{h=i}} &\leq 1,0\ m^3/s \end{aligned} \tag{21}$$

Table 3
Characteristics of reservoirs

Reservoir	Capacity (m^3)	Material	Diameter (m)	Height (m) [min – max level]	Elevation (m)
Covão	40 000	Rock/ Concrete	113	0-4	546
Socorridos	40 000	Rock/ Concrete	113	0-4	76
Santa Quitéria	4 000	Concrete	36	0-4	316

2) The hydropower volume pumped at Socorridos must be balanced daily. This ensures that by the end of each day, the reservoir levels are restored to their starting levels from the beginning of the day.

$$\sum_{h=1}^{24} Q_{tS_{h=i}} \Delta_t = \sum_{h=1}^{24} Q_{pS_{h=i}} \Delta_t \tag{22}$$

3) The volume of water stored in each reservoir must remain above zero and below the maximum capacity specific to each reservoir.

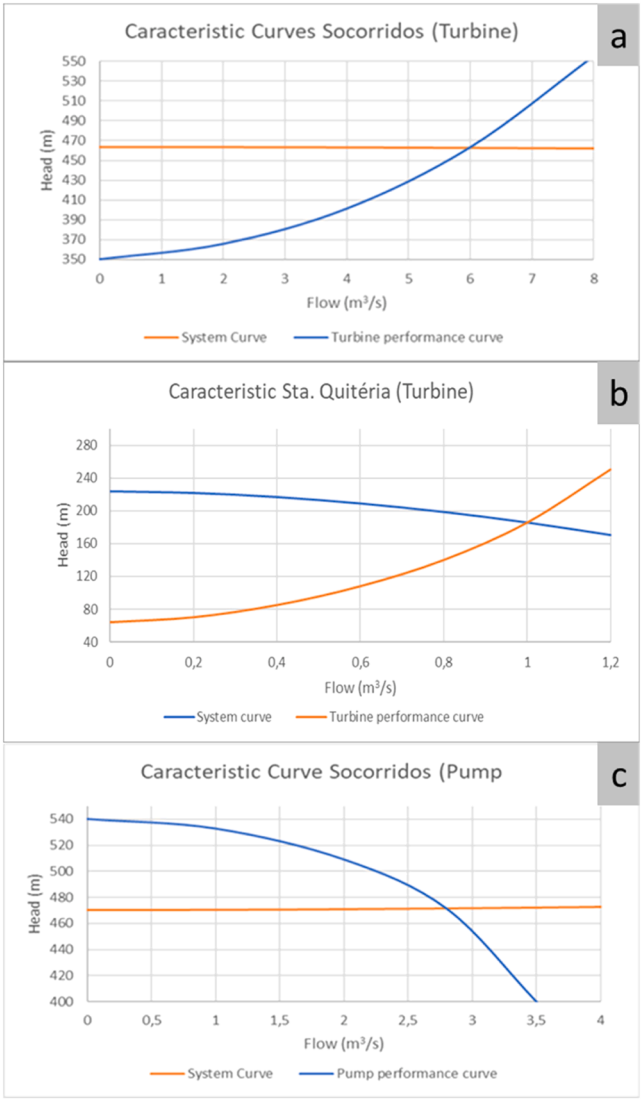

Fig. 4. Characteristic curves for Socorridos and Sta Quitéria: a) Socorridos hydropower; b) Sta Quitéria hydropower; c) Socorridos pump station.

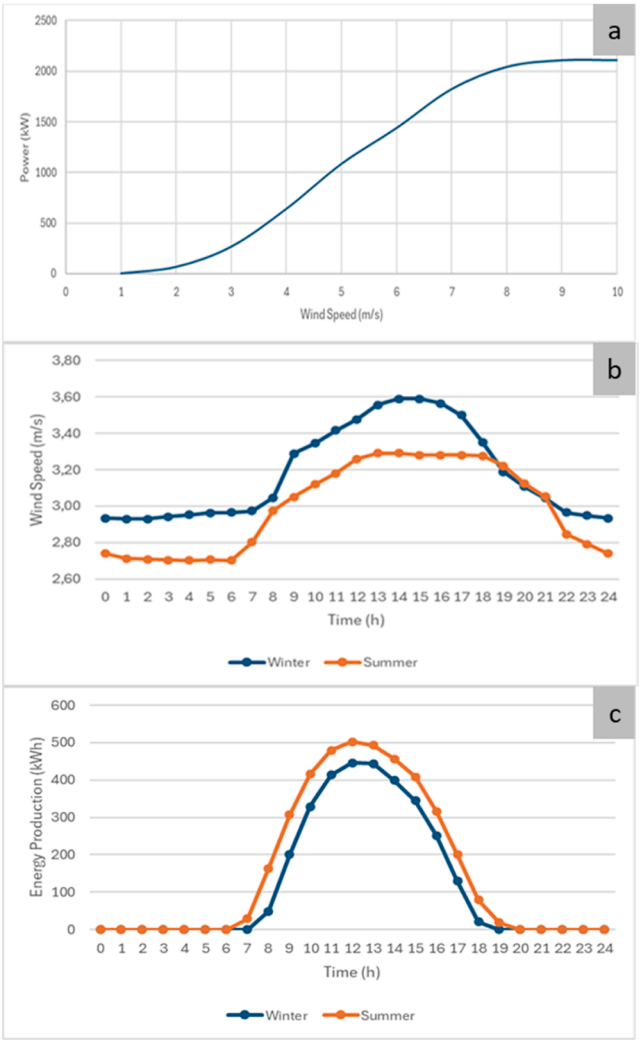

Fig. 5. Wind and solar variation: a) wind speed curve; b) Distribution along 24h and seasons; c) Solar radiation distribution during 24h for the main two seasons

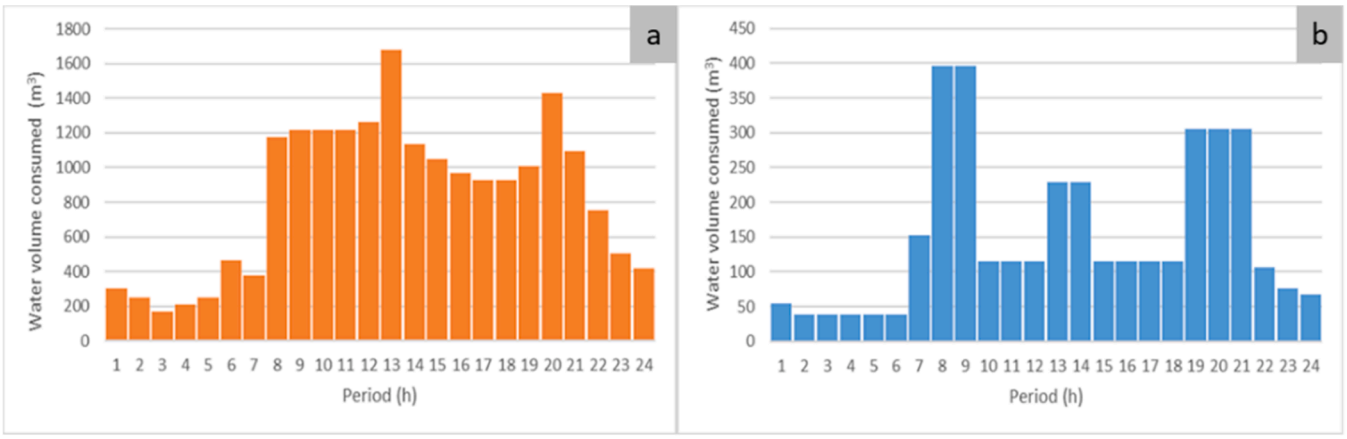

Fig. 6. Daily water consumption volume: a) Covão; b) Santa Quitéria.

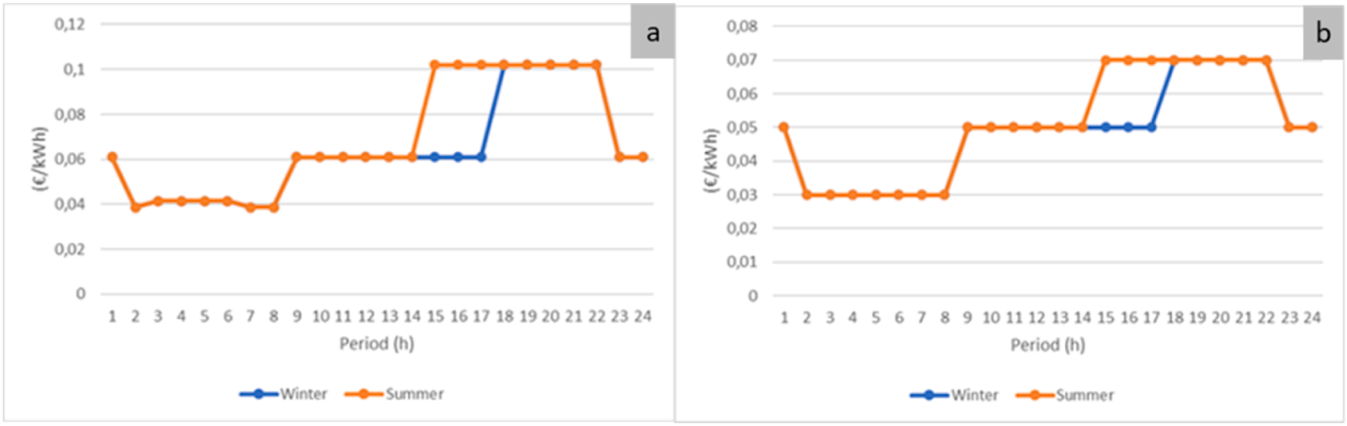

Fig. 7. Energy tariffs: a) buy; b) sell.

$$\begin{aligned} &0\ m^3 \le V_{sC_{h=i}} \le 40000\ m^3 \\ &0\ m^3 \le V_{sS_{h=i}} \le 40000\ m^3 \\ &0\ m^3 \le V_{sSQ_{h=i}} \le 4000\ m^3 \end{aligned} \tag{23}$$

4) For solutions with a daily turbine volume in Socorridos greater or equal to the defined volume (e.g., 40000 m3/day), the initial storage volume in the Socorridos reservoir corresponds to its maximum capacity. For the remaining solutions, the initial storage volume should be equal to its maximum daily turbine volume. This constraint is important to create a cycle every day and to induce the pumping operation during the night when the energy buy tariff is lower.

$$\begin{aligned} V_{sS_{h=1}} &= 40\ 000\ m^3\ if\ \sum_{h=1}^{24} Q_{tS_{h=i}}\Delta_t \gg 40\ 000\ m^3 \\ V_{sS_{h=1}} &= \sum_{h=1}^{24} Q_{tS_{h=i}}\Delta_t \text{if} \sum_{h=1}^{24} Q_{tS_{h=i}}\Delta_t < 40000\ \text{m}^3 \end{aligned} \tag{24}$$

Table 4
Water consumption tariffs

Region	Water Consumption Tariff (€/m³)	
	Winter	Summer
Covão	1.53	1.74
Santa Quitéria	0.77	0.77

5) In the Santa Quitéria reservoir, at the beginning of the day, the water volume storage is never null, to compensate for the deficits registered throughout the entire day.

$$V_{sSQ_{h=1}} \ge 0\ m^3 \tag{25}$$

6) The volume of water stored in the Socorridos reservoir should be zero at the end of the day, to create a cycle that can be repeated daily.

$$V_{sS_{h=24}} = 0\ m^3 \tag{26}$$

7) The water consumption in Covão and Santa Quitéria should be satisfied.

$$\begin{aligned} Q_{dS_{h=i}}\Delta_t &\le Q_{cS_{h=i}}\Delta_t \\ Q_{dSQ_{h=i}}\Delta_t &\le Q_{cSQ_{h=i}}\Delta_t \end{aligned} \tag{27}$$

The ***second scenario*** of optimization is applied, in which only wind turbines are integrated to offset pumping costs. In this case, the objective function is the number of wind turbines required to satisfy the electricity consumption at all times, and the goal is to minimise this function. The constraints associated with this optimization are the same, with an additional restriction to ensure that there is no energy consumption at any time.

$$E_{C_{h=i}} = 0\ kWh \tag{28}$$

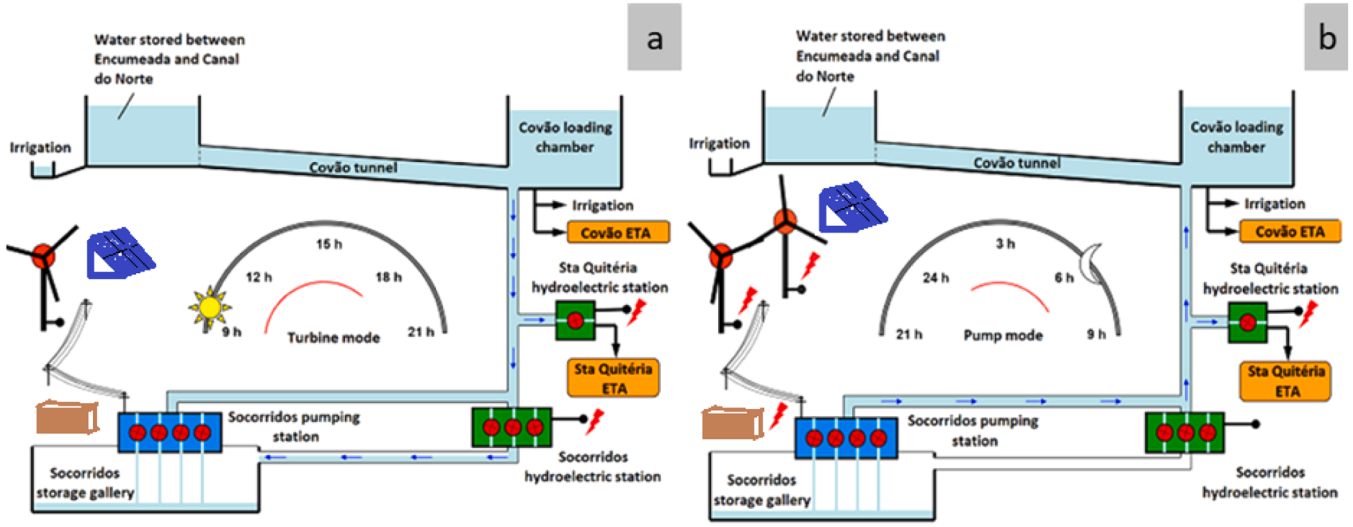

Fig. 8. Types of operation: a) in turbine mode; b) in pump mode

Table 5
Pump and Hydropower: O&M and Investment costs.

Equipment	Location	O&M (€/year)		Investment (€)	
		2025	2030	2025	2030
Pipes	Covão-Socorridos	1 205		120 521	
	Socorridos-Santa Quitéria	2 465		246 505	
Turbines	Socorridos	88 913	82 689	4 445 630	4 134 436
	Santa Quitéria	13 230	12 307	661 481	615 331
Pump	Socorridos	40 385	37 567	2 019 227	1 878 351

Table 6
Wind: O&M and CAPEX

Year	Wind Turbine		PV Solar Panel	
	O&M (€/kWp/year)	CAPEX (€/kWp)	O&M (€/kWp/year)	CAPEX (€/kWp)
2025	21	1228	7.3	330
2030	20	1161	6.2	280

The ***third scenario*** of optimization is used in cases where only PV solar panels are integrated. The objective function is the electricity produced by these devices and sold to the grid. The aim is to maximize this function to exploit the energy potential of the panels since they only produce energy during daylight hours. On the other hand, it is also intended to maximize the NPV, because, in some solutions, the pumping operation occurs during the night.

The ***fourth scenario*** combines the previous but mainly focuses on NPV maximization considering the other criteria associated with the number of energy converters and electricity production.

3.2. Digital twin model

The Socorridos multipurpose system is very complex, and it is necessary to guarantee that the hydraulic conditions are respected, in terms of velocity and pressure. To simulate the effect of the turbines, GPV valve simulators of turbines were placed in Socorridos and Santa Quitéria hydropower plants. After designing the system in EPANET, some simulations were carried out, to understand the variation of velocity and pressure along the entire system to calibrate the model. For each parameter, two different analyses were made, one for the hydropower flow and another for the pumping operation. The simulations were made for the most critical situation, which occurs when the flow rate is maximum. The velocity values obtained for each pipe, for the hydro and pumping flows, respectively (Fig. 9a-b).

As a recommended engineering practice, the maximum velocity in hydropower high-head plants is between 4 m/s and 5 m/s (Ramos and Almeida, 2016). Hence, the velocity in all pipes is near to the recommended values throughout the entire system. In the pipe that links Socorridos and Santa Quitéria, the velocity is zero, when the pumping operation occurs since the Santa Quitéria valve is closed. For pressure, two simulations were also made, one for the hydro and another for pumping flows, as can be seen in Fig. 9c and d, respectively.

4. Results and discussion

4.1. System characteristics and normal operation

This chapter presents the economic results obtained in the Socorridos multipurpose system. Six different solutions were tested, with different hydropower volumes, each of them integrated into four scenarios, that vary in terms of energy source and storage. The hydropower volume and pumped in each solution is represented in Table 7. The hydropower and pumped volumes in Socorridos and Santa Quitéria remain constant throughout the days, as well as the volume used for irrigation in this second location. Santa Quitéria has a constant hydropower volume of 5906 m^3/day and an irrigation volume of 2293 m^3/day.

Covão and Socorridos reservoirs are interconnected, and when the first starts to empty the second starts to fill up. This effect can be shown in Fig. 10, for a daily hydropower volume of 130 000 m^3.

In normal operation, only the hydropower and pump storage systems are active without integrating renewable energies. The pumping operation consumes energy from the grid, with optimisation of pumping and turbine operation periods to maximise the NPV. This scenario does not incorporate the battery to compensate for the pumping costs, because the energy that is produced each day is lower than the energy consumption.

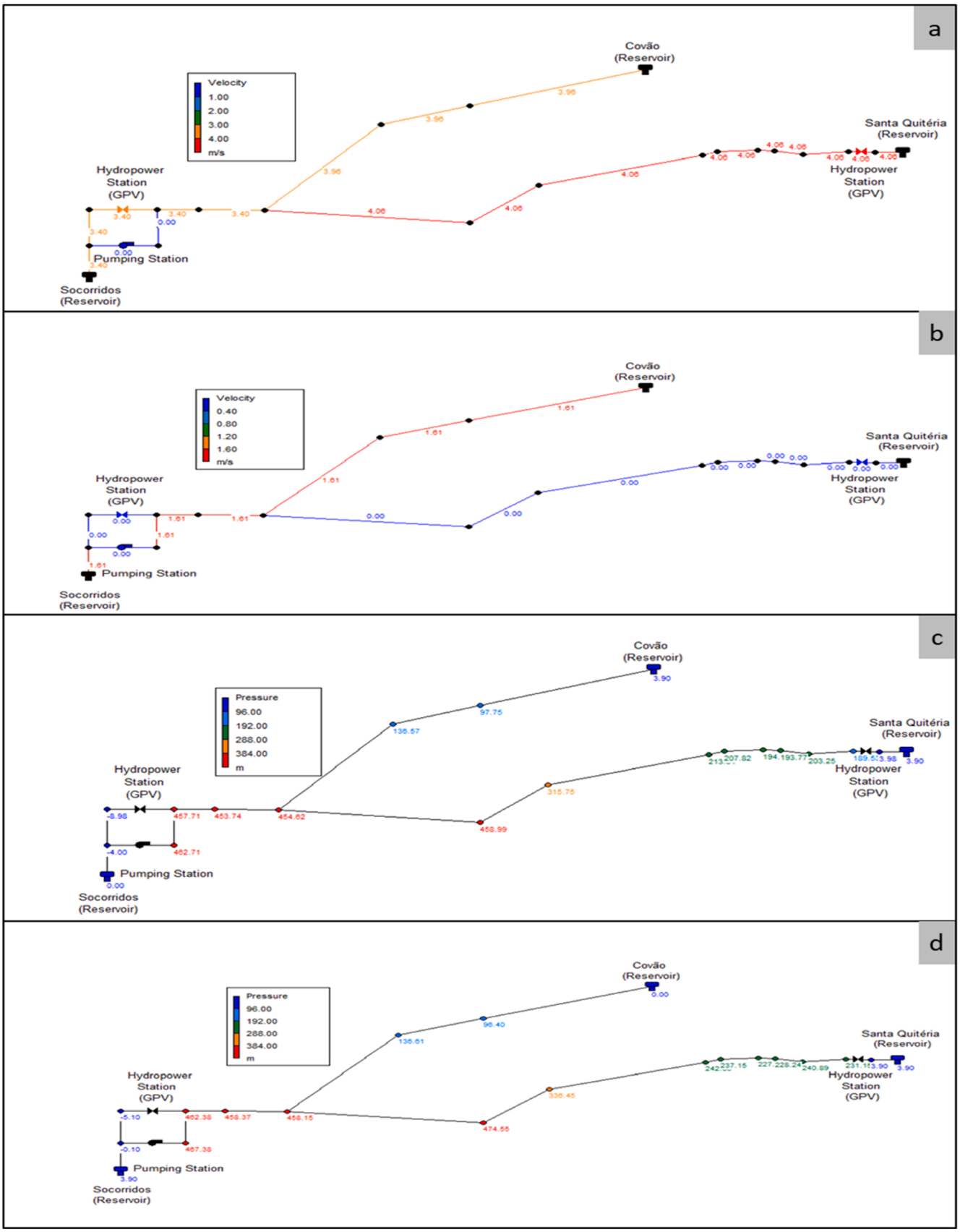

Fig. 9. Flow velocity values: a) for the gravity and b) pumping systems; Pressure values: c) gravity, d) pumping systems

Table 7
Hydropower and pump volumes

Solutions	Volume Hydropower/Pumped (m^3/day)
1	35 167
2	38 260
3	40 000
4	80 000
5	100 000
6	130 000

For the first two solutions, water is pumped during the night when the energy purchase tariff is lower, while water is for hydropower in the Socorridos power plant during the peak energy sale tariff. In solutions 1 and 2, the reservoirs are emptied and filled, consecutively. In the remaining solutions, it is not feasible for the pumping system to operate only at night, as the Covão and Socorridos reservoirs need to be emptied and filled more than once a day. Energy production and consumption are not constant throughout the day.

To calculate the NPV, considered incomes include the benefits from selling energy to the grid and water to the population. Outcomes account for the costs of energy purchased from the grid to satisfy the consumption of pumping water, and the operation and maintenance costs of the pipes and electromechanical equipment. The results obtained for each solution are represented in Table 8.

Analyzing Table 8, it is possible to observe that the isolated operation of the hydropower and pump storage systems is not economically viable, in all solutions, for a lifetime analysis of 20 years. These results can be explained by the high initial investment and the high operating and maintenance costs of turbines and pumps. It is worth mentioning that the pump operation consumes a lot of energy, emitting CO2 into the atmosphere. These emissions correspond to very high taxes, which significantly decreases the NPV. On the other hand, the energy production in Santa Quitéria is very low. However, when the benefits of water distribution are taken into account, all the solutions are very profitable.

The NPV increases until it reaches the optimal result, and then starts to decrease. This phenomenon happens, because for solutions 4, 5 and 6, the Covão and Socorridos reservoirs, are filled and emptied more than once a day, which implies that during some periods the water is turbined in off-peak rate hours, and in opposite the water is pumped in peak rate hours. Another thing that can explain these results, is that for the same amount of water, the energy that is spent to pump the water is higher than the energy that is produced in the turbine, where the energy tariffs have also a relevant influence.

NPV becomes positive in most of the solutions, thanks to the revenues obtained with water supply and water for irrigation in Santa Quitéria. Fig. 11 shows the average percentage of the revenues obtained in each sector.

Hydropower represents a small slice of total revenues, because the flow rates are not very high, and the water distribution and irrigation in these two places are quite significant.

This way, the best solutions occur for daily hydropower volumes in the Socorridos hydropower plant, less than the capacity of the reservoir. In these cases, the reservoirs are filled and emptied only once a day, which allows to turbine of the water in the peak rate hours, and the pumping operation occurs during the off-peak rate hours. These strategies are the only ones, in which the cash flows associated with the hydropower project are positive.

4.2. Solutions of different scenarios

Solutions presented in Table 8 were integrated into four different cases. The first is the normal operation when the water is pumping and hydropower without the aid of additional renewable energies. The second and the third one incorporates wind turbines and solar panels, respectively, to offset the pumping costs. The last scenario contains both devices.

In scenarios that incorporate renewable energies to offset pumping

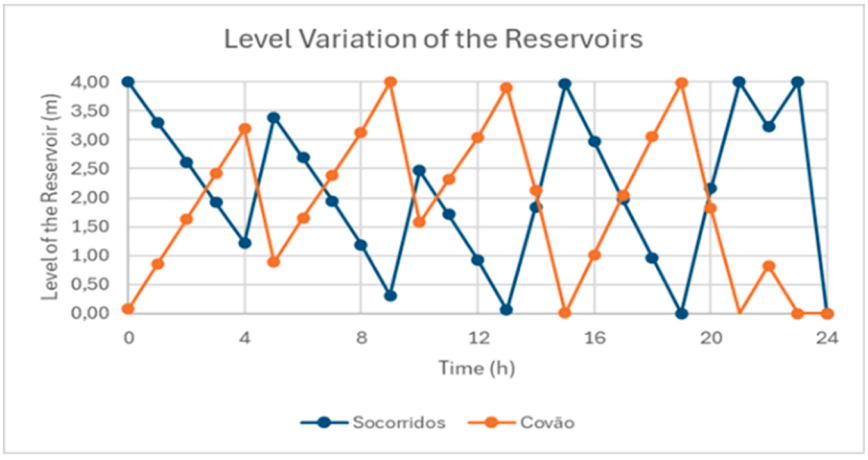

Fig. 10. Level variation of the Covão and Socorridos, for a daily hydropower volume of 130 000 m^3.

Table 8
Energy and NPV estimation without and with profits of water consumption for 2025 and 2030.

Solutions	1	2	3	4	5	6
Energy production Socorridos (kWh/day)	39947	43456	45429	90862	113627	147687
Energy production Santa Quitéria (kWh/day)	3186	3181	3144	2890	2945	2915
Energy consumption Socorridos(kWh/day)	56440	61397	64187	128349	160465	208707
Emissions (kgCO2/year)	18862	20322	21246	42495	53116	69082
NPV 2025 without water consumption (x10^6 €)	-20.03	-21.23	-23.439	-47.911	-57.992	-82.006
NPV 2030 without water consumption (x10^6 €)	-19.405	-20.603	-22.817	-47.289	-57.369	-81.384
Water consumption (m^3/day)	23627					
NPV 2025 (x10^6 €)	150.04	148.42	146.20	121.73	111.65	87.64
NPV 2030 (x10^6 €)	150.24	149.04	146.83	122.35	112.27	88.26

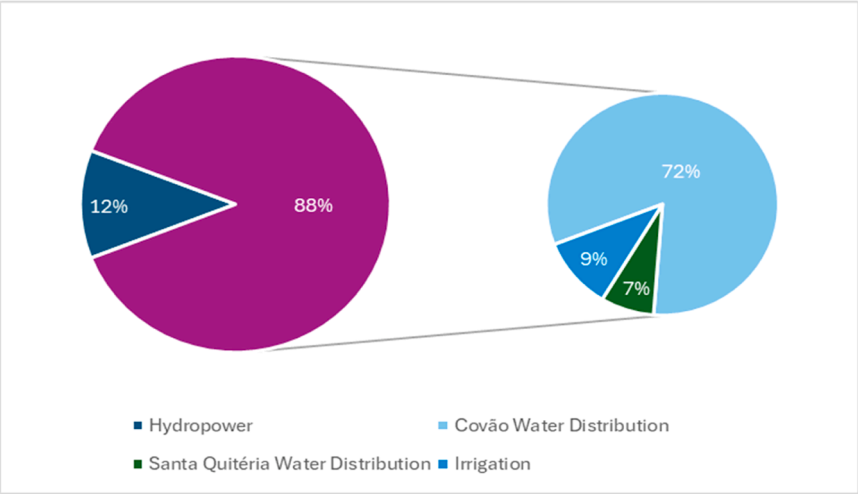

Fig. 11. Distribution of the revenues in the total NPV

costs, the pumping period was selected to minimize energy consumption from the grid and the number of devices required. Consequently, the variation in the level of the Socorridos reservoir throughout the day differs for each solution and scenario. Only the results for the Socorridos reservoir will be presented, as there is no water consumption, and the variation in its level reflects the pumping and hydropower periods. Fig. 12-a,b,c,d, shows the variation in the Socorridos reservoir level with a hydropower volume equal to 40000 m3, the energy consumption by the pump, and the energy available provided by each type of renewable energy.

Analyzing Fig. 12, it is possible to observe that for the same hydropower volume, the hydropower operation is always at the end of the afternoon, when the energy sell tariff is higher. However, the pumping periods are not equal in these four scenarios. In scenario 1, with only the Hydropower, the Socorridos reservoir empties overnight, when the energy buy tariff is lower. For scenario 2, the Wind in Madeira Island is higher at the end of the day and makes it possible to produce a considerable amount of energy during the day. This way, the water is pumping during the day, being the most significant part pumped at the end of the afternoon. Scenario 3, incorporates Solar and Hydropower, and the energy is mostly pumped in the sunshine hours. In scenario 4, which incorporates all the sources of renewable energy, the pumping operation is very similar to the obtained in scenario 3, with the slight difference that in this case, part of the water is pumping in the early morning and at the end of the day in scenario 3, when the solar radiation is lower. This is possible, thanks to the contribution of wind turbines. It should also be noted that there is no great difference in the periods in which sources of renewable energy produce energy for summer and winter, and the peak period of production also occurs mostly at the same time. For the maximum daily hydropower volume (130 000 m3), the Socorridos system behavior is represented in Fig. 13 for different scenarios.

For the maximum daily hydropower volume, the Socorridos reservoir fills and empties more than once a day. In these cases, the operation is only possible with the maximum flow rate in hydropower and pump storage, because this volume corresponds to the maximum volume of water that is possible to move between Covão and Socorridos every day. The peak of energy consumption occurs in the same hours. However, this peak occurs several times a day, because it is impossible to restrict the maximum consumption in hours when the energy provided by renewable sources is maximum. For the solution of Fig. 13 b), the wind energy production hits reasonable values, during the day, which allows to satisfy the consumption in all the hours. In Fig. 13c), the energy consumption occurs mostly during the sunshine hours, and in this case, three peaks of energy consumption occur during this period. These solutions are unable to fully satisfy the consumption, and a large part of the consumption occurs during hours when there is no solar energy production Finally, for scenario 4, with hydro, wind, and solar power, one of the peaks occurs in a period when the solar energy production is maximum. In the summer, wind power cannot meet the consumption during these hours, but ample solar energy is available at this time, to compensate for the gaps.

It is challenging to compare these solutions, in scenarios that incorporate renewable energies, because the number of wind turbines or solar panels is not constant for all the solutions. The best solution depends, on the adopted criteria.

With these results, the aim is to choose the most economically viable solution that fulfills the necessities in terms of consumption, hydraulic requirements, space occupied by renewables, and if it is possible the minimum CO2 emissions (avoiding energy grid purchase).

4.3. *Solutions without batteries*

This section shows the results obtained for scenarios (2, 3 and 4) that do not include batteries to store the excess of energy when it incorporate renewable energies (wind turbines and solar panels) to offset the pumping costs. In all of these solutions the aim is to maximize the NPV, and at the same time minimize the number of devices required to create a system with minimal energy consumption from the grid.

It was adopted the maximum number of solar panels that are possible to set up in the selected zone. On the other hand wind turbines are more expensive, and it is not necessary to install all the wind turbines, to satisfy the pump consumption. For this reason, it was tried to minimize the number of these devices. Fig. 14a shows the number of wind turbines installed for each solution in Scenarios 2 and 4.

The integration of solar panels, in Scenario 4, allows to reduce the number of wind turbines required, compared with the results obtained in Scenario 2. In the first solution (Volume min), the reduction is more significant, because the solar panels can offset the majority of the energy consumption.

Fig. 14b, shows the initial investment, made before the start of the operation of the system, for each scenario and solution, in 2025 and 2030. The initial investment includes all the CAPEX, associated with the electromechanical equipment (wind turbines, solar panels, hydro turbines and pumps) and in the replacement of the pipes.

As expected, the initial investment increases when the daily hydropower volume increases, because more devices are needed to satisfy the energy consumption. The solutions that incorporate only solar panels are the ones with lower initial investment. This can be explained, since these devices are cheaper per kWh than wind turbines, and on the other

hand, the number of devices implemented is insufficient to satisfy all the pumping costs. It is also important to emphasize that the initial investment is the same for all the solutions because the number of solar panels is equal in each solution.

The incorporation of solar panels in Scenario 4, reduces, in the majority of the cases, the initial investment. The moment, when the operation starts, is very important because the prices of the equipment tend to decrease very fast in the next 5 years. It is estimated that the high price reduction of solar panels has already taken place in recent years, contrary to wind turbines. The difference in prices increases when the

Fig. 12. Scorridos system behavior with renewable hybridization and percentage of pumped-storage hydropower operation, for V= 40 000 m3: a) Hydro operation; b) Example of daily operation for hydropower; (c) Hydro+wind operation; (d) Daily operation for hydro+wind; (e) Hydro+PV; (f) Daily operation for Hydro+PV; (g) Hydro+Wind+PV; (h) Daily operation for all sources.

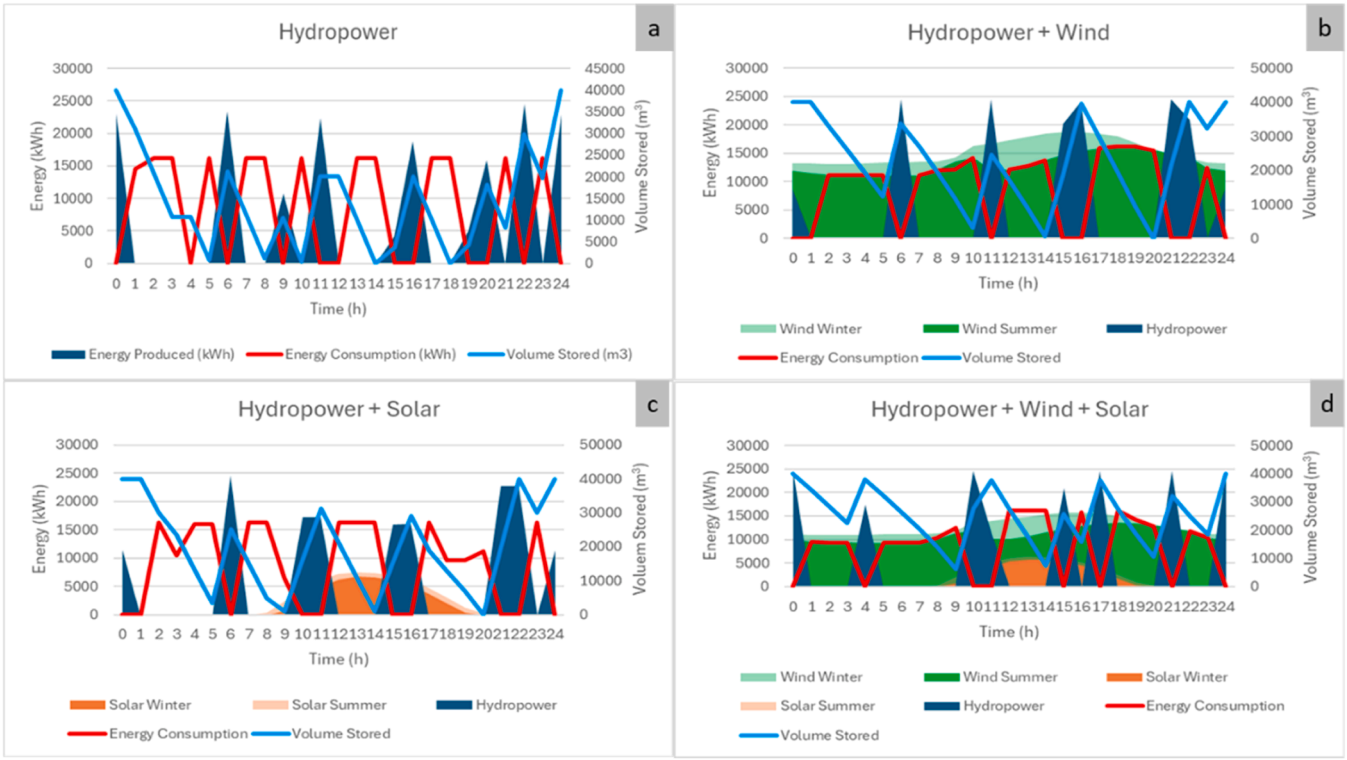

Fig. 13. Scorridos system behavior with energy consumption to pump, for V= 130 000 m3 and different renewable sources: a) Hydro; (b) Hydro+wind; (c) Hydro+Solar; d) Hydro+Wind+Solar.

daily hydropower volume also increases, and in the last solution, it is possible to observe differences of around 12 million euros.

Beyond the investment costs, a critical factor significantly impacts the Net Present Value (NPV) is the quantity of energy sold to the grid, as it constitutes a substantial benefit of the system. An increase in the volume of energy sold correlates directly with a higher NPV. Fig. 14c and d illustrate the daily energy consumption (C) and the daily energy generated (G), for winter and summer. The difference between these two

Fig. 14. Number of wind turbines installed for Scenarios 2 and 4 for different hydro volumes; (b) Initial investment in 2025 and 2030, for each solution; (c) Daily energy consumption(C) and generated (G) for each solution in winter; (d) Daily energy consumption (C) and generated (G) for each solution in summer.

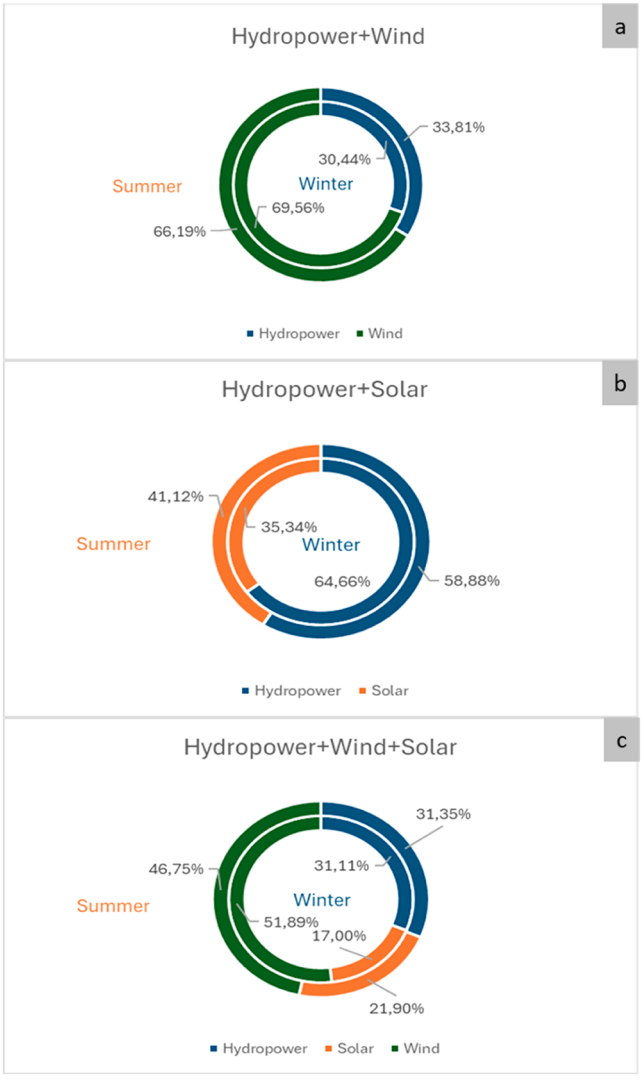

Fig. 15. Average Energy generated by each source of energy, in winter and summer: a) Hydro+wind; b) Hydro+Solar; c) Hydro+wind+solar.

variables represents the amount of energy available for sale to the grid daily and encompasses energy from all types of alternatives, including hydropower, wind, and solar.

The integration of these two types of devices, i.e., wind and solar, allows in some cases, harnessing solar energy to pump the water and the useless wind energy to sell the energy to the grid throughout the day. This scenario is only possible for daily lower hydropower volumes. Fig. 15 represents the percentage of the average energy generated by each source of energy.

Wind power represents a large percentage of the total energy produced by the system, only using the minimum number of wind turbines. These devices have the capability of generating large amounts of energy, and in solutions with high daily hydropower volumes, there exists a considerable number of wind turbines, and the wind power can produce approximately two times more energy than hydropower. Contrary to wind power, solar power produces less energy than hydropower. In this last case, the difference between seasons is more significant, with a reduction of 5% during winter compared with summer. Solutions that integrate the three sources of energy, wind power continues to represent the highest percentage both in winter and summer. However, there is a significant reduction in energy production by these types of energy (Scenario 4) compared with the scenario 2. This can be explained by the fact that solar power can offset part of energy production, especially during summer, when wind efficiency is lower and solar efficiency is higher.

Fig. 16 illustrates the average percentage of energy produced by wind turbines and solar panels that is utilised for pumping and sold directly to the grid. In scenarios involving hydropower and solar, all the energy generated by the solar panels is dedicated to pumping. However, solar power alone is insufficient to meet consumption demands. Consequently, for this scenario, a graph has been created to depict the energy consumed by the solar panels and the energy consumed from the grid.

Analyzing Fig. 16(a), it becomes evident that in Scenario 2, the system designed with the minimum number of wind turbines is capable of generating a significant amount of energy for sale to the grid, particularly during the winter months. In Scenario 3, the energy consumption from the grid to support pump operations is notably substantial. During winter, it accounts for more than half of the total energy consumption, which significantly decreases the NPV of these solutions. Based on this data, it is estimated that, on average, an area of solar panels two to three times larger than initially designed would be required to satisfy the entire energy consumption in this scenario. Lastly, in Scenario 4, the integration of both energy sources facilitates the sale of energy generated by both wind turbines and solar panels. A significant reduction of 10%, is registered in the use of wind turbines for

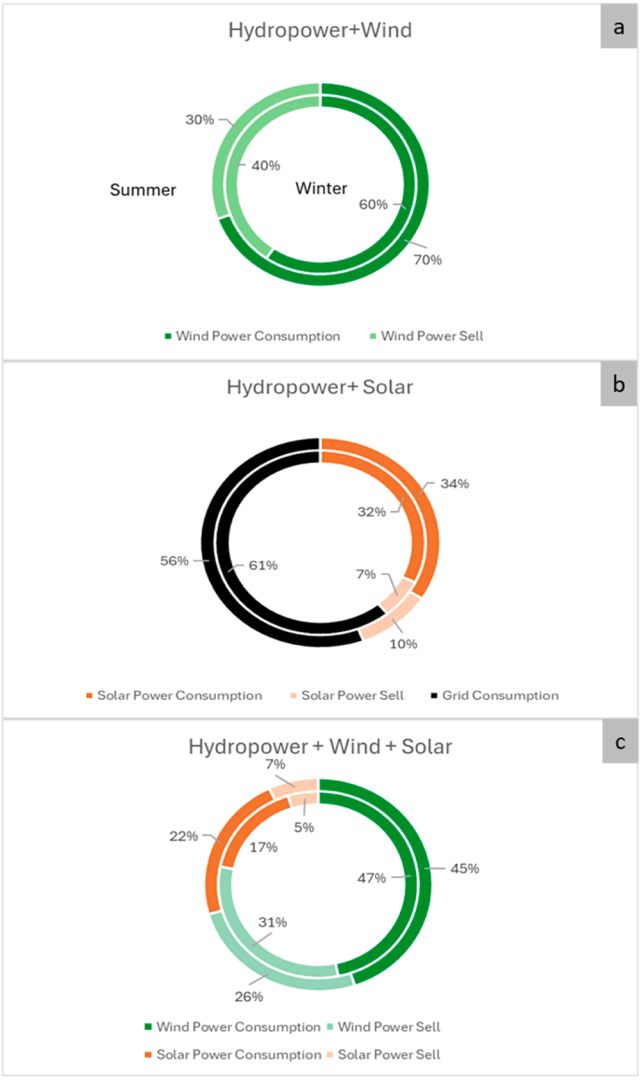

Fig. 16. Average Energy sold by each source of energy, in winter and summer: a) Hydro+wind; b) Hydro+Solar; c) Hydro+wind+solar.

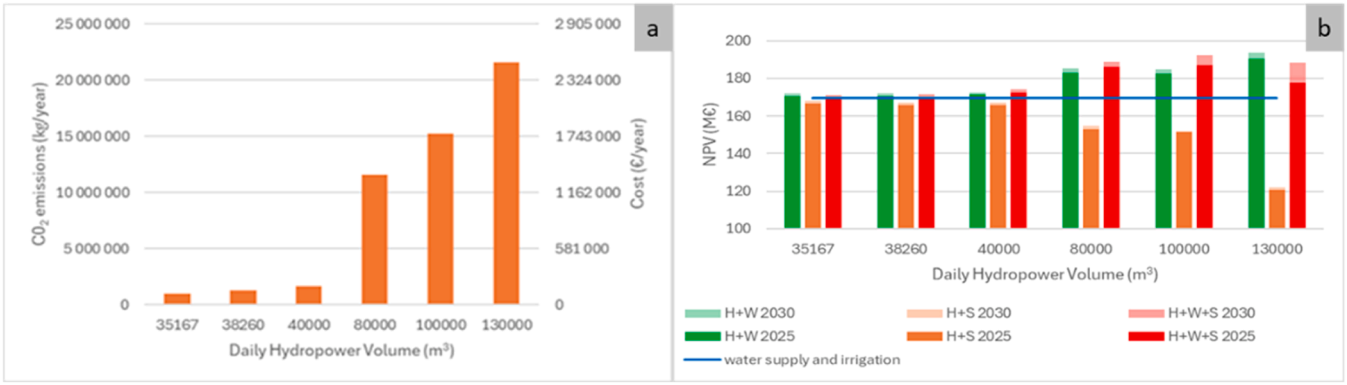

Fig. 17. (a) CO2 emissions, and the costs associated with the emissions for solutions of Scenario 3; (b) NPV in 2025 and 2030, for each solution.

consumption and selling energy to the detriment of solar power.

The buying of energy to the grid, to satisfy the demand, in Scenario 3, involves C02, because the energy consumption does not come from renewable sources. These emissions are taxed, increasing the costs, and can be calculated using Eq. (18). Fig. 17a shows the CO2 emissions and the costs associated with its emissions for each solution present in Scenario 3.

For the first three solutions, the emissions are not significant, because the number of solar panels implemented is sufficient to offset the majority of the consumption. However, when the daily hydropower volume increases, a large part of the energy is consumed from the grid, which represents a huge annual cost.

Based on the results presented it was possible to calculate the NPV for each solution in two different years, 2025 and 2030 (Fig. 17b). In this case, the benefits include the profit from selling energy to the grid and the income from water distribution and irrigation. On the other hand, the costs include all expenses related to the operation and maintenance of the equipment and pipes, and in some solutions the costs associated with CO2 emissions.

Fig. 17b shows that scenario 3, which incorporates only solar panels, to offset the pumping costs, never corresponds to the best result in each solution. However, in the first three solutions, the NPV for this scenario is very close to the other scenarios, because the solar panels can satisfy the majority of the pump consumption. The major part of the benefits is provided by water supply and irrigation, as can be seen with the blue line in Fig. 17b. For the solutions of scenario 3, the NPV is always below the NPV of water supply and irrigation, which means that these hydropower and pump-stored projects generate losses, and are less economically viable. In the remaining solutions, the NPV is always above the NPV of water supply and irrigation, which indicates the production of energy generates benefits that increase the NPV, making these solutions profitable.

4.4. Solutions with batteries

This chapter will present the results obtained for scenarios (2, 3 and 4), including batteries to store the excess of energy. In these types of solutions, it is possible to create a system with a minimum waste of energy and make it more independent of the grid. To simplify the calculations and to allow a comparison with the previous results, the same pump operation was adopted. The objectives of the optimizations are also the same, however, the number of devices can be different in some solutions.

A larger number of solar panels is needed to satisfy the pump consumption, however, the space is limited to 5 hectares. To maximize the potential of this type of energy, it was also adopted the maximum number of solar panels, associated with each scenario. The number of wind turbines used was calculated using the Eqs. (29) and (30). In scenario 2 that do not include solar panels, the portion of energy production associated with these devices is zero.

$$N_{Wind\ turbines\ seasson} = \frac{\sum_{h=0}^{24} E_{consumption\ h} - \left(\sum_{h=0}^{24} E_{Solar\ panel\ h} \times N_{sollar\ pannels}\right)}{\sum_{h=0}^{24} E_{P\ Wind\ turbine\ h}} \tag{29}$$

$$N_{wind\ turbines\ adopted} = max\left(N_{Wind\ turbines\ winter}; N_{Wind\ turbines\ summer}\right) \tag{30}$$

After these calculations, the number of wind turbines associated with each solution was determined (Fig. 18a).

To store the energy, larger batteries can be installed, in different sizes. The energy can be stored to be used later in the pumping operations or to be sold in periods when the energy sell tariff is higher, to increase the benefits. In cases where there exists a negative balance between the energy produced and the energy consumption, there must be enough energy stored at the start of the day, to compensate for these

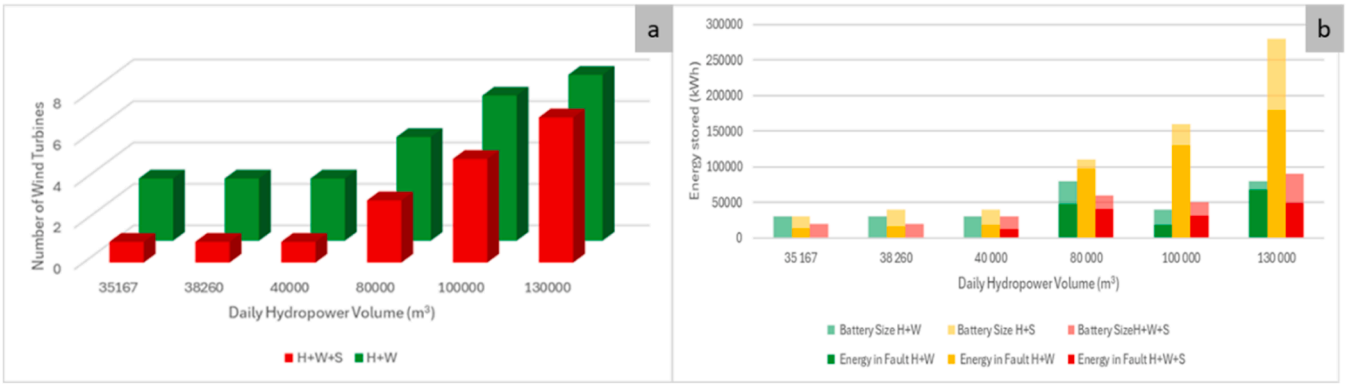

Fig. 18. (a) Number of wind turbines installed for Scenarios 2 and 4; (b) Size of the battery and energy in fault for each solution

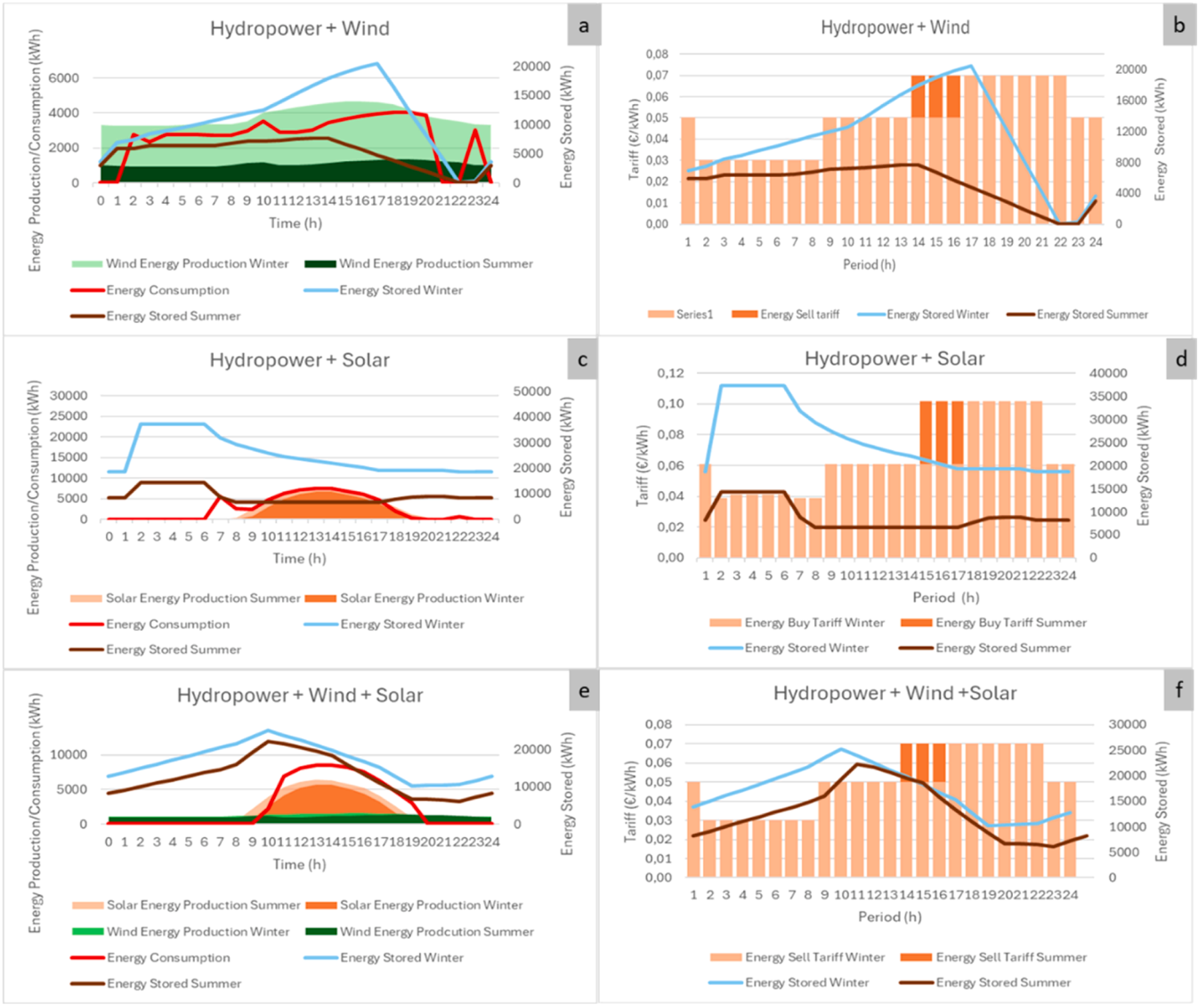

Fig. 19. Solution 3: (a) With batteries: Energy Production, Consumption, and Stored for Hydro+Wind; b) Correlation between energy stored with buy and sell tariffs for Hydro + Wind; (c) Energy Production, Consumption, and Stored for Hydro+Solar; d) Correlation between energy stored and buy and sell tariffs for Hydro+Solar; (e) Energy Production, Consumption and Stored for Hydro+Wind+Solar; (f) Correlation between energy stored with buy and sell tariffs for Hydro+Wind+Solar

deficits. Fig. 18b shows, the size of the batteries adopted for each solution and the amount of energy stored in the batteries at the start of the day, when there exists a negative balance of at least one hour a day. Another important conclusion, after analysis of Fig. 18, is that the size of the batteries does not vary linearly with the daily hydropower volume.

Fig. 19a represents, the relation between energy production, energy consumption, and the energy stored. In Fig. 19b, the relation between energy stored and buy and sell tariffs. It was presented the three scenarios, each of them for the solution that has a daily hydropower volume equal to 40 000 m3.

Fig. 19a shows that energy consumption consistently remains below energy production across both seasons. Consequently, the battery is primarily used to store energy for future sale. In Fig. 19b, energy storage begins to decrease when the energy selling tariff reaches its maximum, indicating that energy is sold during this period. This selling period is extended in the summer, resulting in an earlier decrease in stored energy for this season.

When only solar panels are used to cover pumping costs, Fig. 19c reveals that the energy consumption curve occasionally exceeds the energy production curve. Despite this, energy consumption remains below the total energy stored at any given time. In such scenarios, additional energy must be purchased from the grid to meet consumption needs. This occurs when the energy purchase tariff is at its lowest, leading to an increase in stored energy (Fig. 19d).

Fig. 19e illustrates a scenario that combines aspects of the previous solutions. In this case, energy consumption is higher than energy production during certain hours but remains lower than the stored energy. Unlike the previous solution, there is no need to purchase additional energy from the grid, as excess energy not used for pumping is stored in the battery. Stored energy is utilized to address both scenarios presented earlier, and energy sales commence when the selling tariff is at its peak (Fig. 19d). It is important to note that there are instances when energy consumption can exceed the amount of stored energy, occurring only when consumption surpasses the difference between current energy consumption and stored energy.

Based on the provided data, the initial investment required for each solution can be calculated for the years 2025 and 2030, as shown in Fig. 20a.

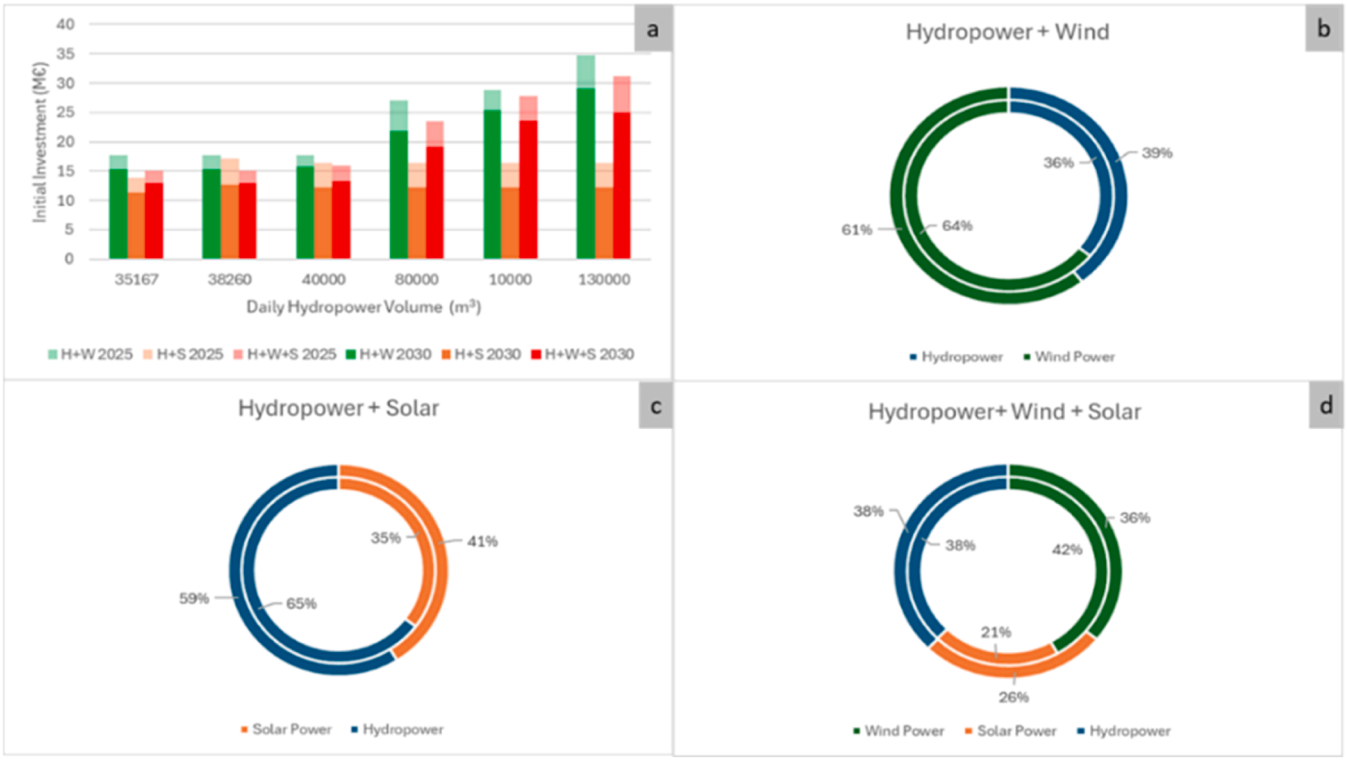

Fig. 20. (a) Initial Investment for 2025 and 2030; (b) Energy production for Hydro + Wind; (c) Energy production for Hydro + Solar; Energy production for Hydro + Wind + Solar.

The initial investment is highly sensitive to battery costs, as evidenced by the significant variation observed between the two analyzed years. This difference is largely driven by the anticipated sharp decline in battery prices in the near future, a result of the accelerating energy transition. The integration of batteries alters the distribution of energy generation among different sources, as illustrated in Fig. 20b-d.

Similar to systems without battery integration, the proportion of energy generated by each source fluctuates seasonally. Wind power contributes a larger share during the winter months, while solar energy dominates during the summer. In Fig. 20b, a reduction in the number of wind turbines leads to a decrease in wind energy generation, which consequently increases the proportion of energy produced by hydropower. In Scenario 3 (Fig. 20c), the energy mix remains consistent with non-battery solutions, as the number of solar panels remains constant.

In Scenario 4 (Fig. 20d), hydropower maintains a consistent contribution throughout both the winter and summer. The inclusion of batteries enables solar energy to play a more prominent role in overall energy production, particularly during the summer months. However, as observed in Fig. 20b, the significance of wind power diminishes, resulting in a more balanced contribution from each energy source during the summer. Fig. 21 presents the average percentage of electricity used for pump operation and the amount sold back to the grid.

Fig. 21a illustrates that the majority of the energy produced by wind turbines is utilized for pumping operations. The energy sold to the grid represents the surplus not required for pumping, and this percentage is lower in both winter and summer compared to the same solutions without battery integration. This reduction is primarily due to the lower number of wind turbines employed in these scenarios. In solutions that rely solely on hydropower and solar energy (Fig. 21b), all the energy generated by solar panels is allocated to pump consumption. As a result, compared to similar solutions, the amount of energy that needs to be purchased from the grid to support pump operations is reduced.

In Fig. 21, wind power continues to contribute a higher proportion of energy compared to solar panels. However, in contrast to non-battery solutions, the use of solar energy for consumption increases, while the contribution of wind power decreases. Each of the cases presented in Fig. 21 demonstrates that the energy produced is utilized more efficiently, resulting in a lower amount of energy available for sale to the grid. This operational mode leads to a reduction in the overall costs of the solutions and lowers potential profits.

Fig. 22a presents the CO2 emissions associated with each solution, along with the corresponding monetary costs of these emissions.

Even though, with the integration of batteries, the grid energy consumption has decreased, a lot of C02 emissions continue to be emitted every year, especially for solutions with high daily hydropower volume. These emissions are taxed, and represent an enormous cost every year, which decreases the NPV, and makes the solutions economically less attractive (Fig. 22b).

High hydropower volumes require large batteries, increasing costs, as these solutions only supply energy for pumping. In contrast, wind-integrated solutions continuously produce energy, sell excess to the grid, and require smaller batteries, making them more economically attractive. Scenario 3 presents a NPV lower without batteries, making turbine and pump installations less feasible. For high hydropower volumes, wind-integrated solutions in Scenario 4 show a significant NPV advantage.

4.5. *Comparison between battery and non-battery solutions*

The solutions that incorporate batteries or do not exhibit the same pump storage and hydropower operations. However, some differences can be noticed in terms of the number of wind turbines necessary to satisfy the consumption, the initial investment, and the emission of CO2. All these factors have an enormous influence on NPV. The integration of batteries allows the storage of the energy to be used later, reducing the excess of energy and the number of wind turbines (see Fig. 23a).

The difference in the initial investment between battery and non-battery solutions for each scenario is illustrated in Fig. 23b. Generally,

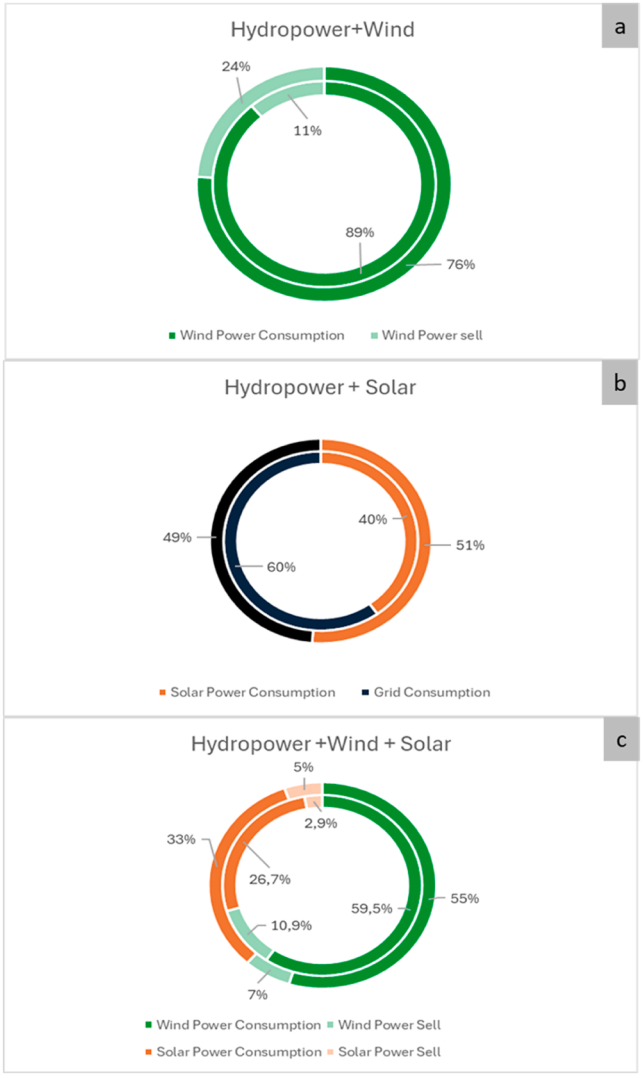

Fig. 21. Contribution of each source of energy (Wind and Solar) for energy consumption and energy sell a) Hydro + Wind b) Hydro + Solar c) Hydro + Wind + Solar

for low daily hydropower volumes, battery-integrated solutions are more costly. In scenarios that incorporate wind turbines, the initial investment decreases with higher daily hydropower volumes, primarily due to the reduced number of wind turbines required and the anticipated affordability of batteries by 2030. In contrast, solutions that rely solely on hydro and solar power become less advantageous with battery integration, as there is no reduction in the number of solar panels required to meet pump energy demands. However, these solutions do benefit from a reduction in grid energy purchases, which has a direct impact on CO2 emissions and associated costs (Fig. 23c). Battery integration leads to a decrease in emissions, and subsequently, a reduction in related costs (Fig. 23d). Despite the reduction in emissions, they remain substantial for high daily hydropower volumes, leading to significant costs that lower the Net Present Value (NPV) and diminish the economic viability of these solutions. The differences in NPV between battery and non-battery solutions in 2030 for each scenario are shown in Fig. 23d.

5. Conclusions

A new methodology for optimizing hybrid renewable water supply systems using digital twin technologies and a multicriteria approach was developed, focusing on isolated cities like Madeira Island. This study designed six different solutions based on hydropower volumes, water-energy consumption, and renewable energy integration scenarios. The results show that solutions relying solely on solar panels generate less energy than those incorporating wind turbines, due to the insufficient number of solar panels to meet energy demands. In high hydropower scenarios, the energy output from solar-only systems is often insufficient to operate pumps, making them less economically viable.

The inclusion of wind turbines significantly enhances the system's energy output, generating excess energy that can be sold to the grid. This surplus energy helps improve the economic viability of the system, particularly when hydropower volumes are large. Wind turbines provide a steady energy supply throughout the day, unlike solar panels, which are limited to daylight hours. Consequently, wind turbines allow for more flexible pumping schedules and maximize the potential for energy sales, boosting the NPV.

Scenarios with large daily hydropower volumes and no battery storage reveal that integrating wind turbines (Scenarios 2 and 4) is the most economically viable option due to the excess energy available for sale. In contrast, solar-only systems see reduced NPV as hydropower demands increase, requiring additional grid energy for pumping. The study finds that two wind turbines outperform 12,823 solar panels, especially for hydropower volumes of 130,000 m^3/day. Notably, NPV differences between 2025 and 2030 are minimal, with initial investment costs having the most significant impact.

When batteries are incorporated, wind turbine solutions don't require large battery storage initially, as the turbines produce excess energy that can be stored and sold during peak tariff periods. However, as hydropower volumes increase, battery size must grow, particularly for solar panels, which depend on energy storage due to limited direct energy production. Battery integration generally reduces NPV for solar-only solutions, as the cost of purchasing energy and storing it during off-peak periods outweighs potential profits from grid sales. Wind turbine

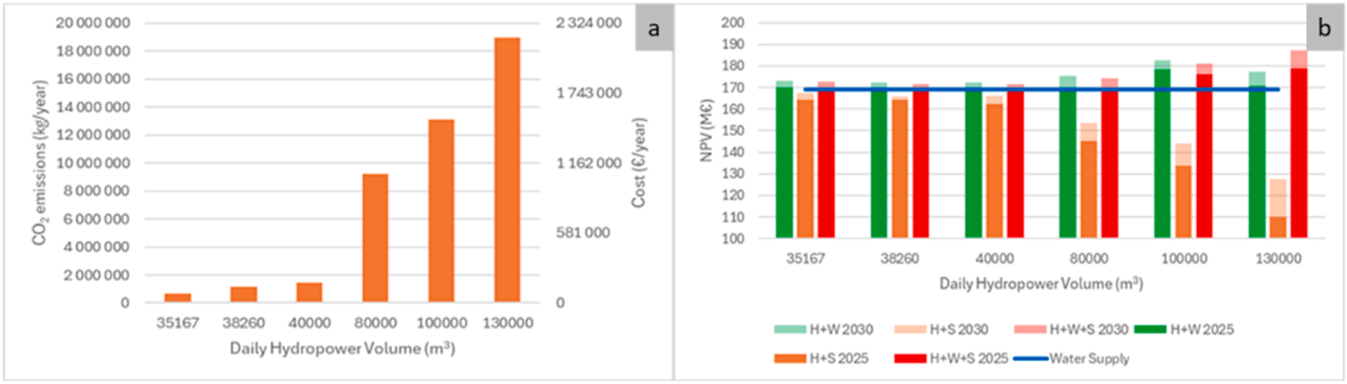

Fig. 22. CO2 emissions: (a) CO2 emissions by each solution and the emissions costs; (b) NPV in 2025 and 2030, for battery solutions

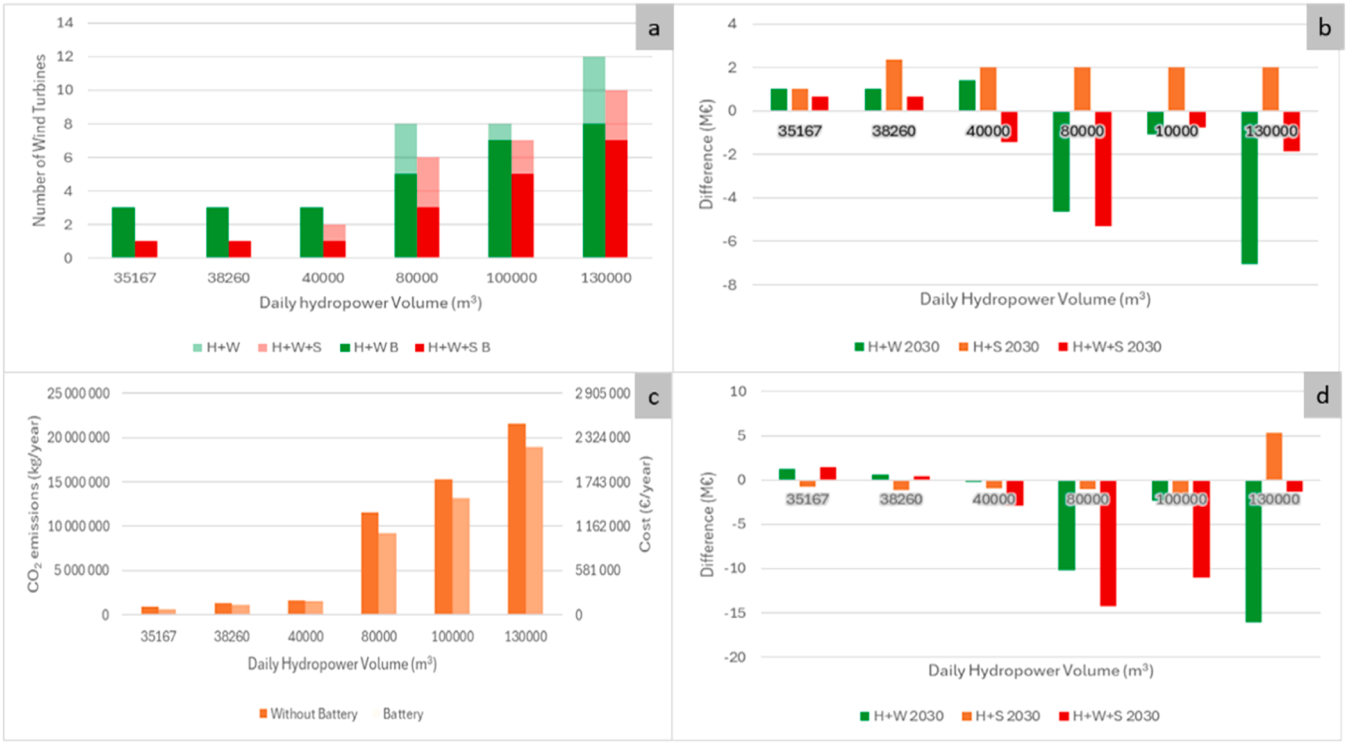

Fig. 23. (a) Number of wind turbines, for battery and non-battery; (b) Initial investment difference between battery and non-battery in 2030; (c) CO2 emissions and the respective costs, for battery and non-battery solutions; (d) NPV difference between battery and non-battery in 2030

solutions also experience a decrease in NPV with battery integration, as the reduced number of turbines lowers the amount of energy available for sale.

Comparing solutions with and without batteries reveals that for low daily hydropower volumes, the number of wind turbines remains the same, as most of the energy produced is used for consumption. However, for high hydropower volumes, fewer wind turbines are required when batteries are used, as excess energy is avoided through storage. While this reduction lowers initial investments, it also decreases energy sales, impacting NPV. In summary, solar-only solutions are less attractive for high hydropower volumes, wind turbine integration enhances energy output and profitability, and adding batteries typically reduces NPV by decreasing energy sales and increasing costs.

CRediT authorship contribution statement

Miguel Tavares: Writing – original draft, Methodology, Investigation. **Modesto Pérez-Sánchez:** Writing – original draft, Methodology, Investigation, Conceptualization. **Armando Carravetta:** Writing – review & editing. **Oscar E. Coronado-Hernández:** Writing – review & editing, Formal analysis. **P. Amparo López-Jiménez:** Writing – review & editing. **Helena M. Ramos:** Writing – original draft, Supervision, Funding acquisition, Formal analysis, Conceptualization.

Declaration of competing interest

The authors declare that they have no known competing financial interests or personal relationships that could have appeared to influence the work reported in this paper.

Data availability

Data will be made available on request.

Acknowledgement

This work was supported by FCT, to UIDB/04625/2020 CERIS, in the Hydraulic Laboratory, for experiments on Pumped-storge and hydropower, and the project HY4RES (Hybrid Solutions for Renewable Energy Systems) EAPA_0001/2022 from INTERREG ATLANTIC AREA PROGRAMME. Part of the research was carried out during Modesto Pérez-Sánchez's stay at the CERIS-IST research center, called "INCORPORATION OF NEW WATER RESOURCES IN IRRIGATION SYSTEMS THROUGH THE USE OF SUSTAINABLE TECHNOLOGIES AND COMPUTATIONAL TOOLS TO MITIGATE WATER SCARCITY".

Fundings

Funding for open access charge: CRUE-Universitat Politècnica de València. Project HY4RES (Hybrid Solutions for Renewable Energy Systems) EAPA_0001/2022 from INTERREG ATLANTIC AREA PROGRAMME and Grant PID2020-114781RA-I00 funded by MCIN/AEI/10.13039/501100011033.

References

Abdalla, A., El-Osta, W., Nassar, Y. F., Husien, W., Dekam, E. I., & Miskeen, G. M. (2023). Estimation of dynamic wind shear coefficient to characterize best fit of wind speed profiles under different conditions of atmospheric stability and terrains for the assessment of Height-Dependent Wind Energy in Libya. *Appl. Sol. Energy (English Transl. Geliotekhnika), 59*, 343–359. https://doi.org/10.3103/S0003701X23600212/FIGURES/21

Ahmed, A.A.; Alsharif, A.; Khaleel, M.; Nassar, Y.F. Integrating Renewable Energy Sources with Electric Vehicle Infrastructure for Enhanced Renewability., doi :10.4108/eai.5-1-2024.2342575.

Ahmed, A.A.; Alsharif, A.; Khaleel, M.; Nassar, Y.F. Strategic Renewable Energy Source Integration for Charging Stations in Plug-in Hybrid Electric Vehicle Networks., doi :10.4108/eai.5-1-2024.2342576.

Akrofi, M. M., & Okitasari, M. (2022). Integrating solar energy considerations into urban planning for low carbon cities: A systematic review of the state-of-the-art. *Urban Gov, 2*, 157–172. https://doi.org/10.1016/J.UGJ.2022.04.002

Alhasnawi, B. N., Almutoki, S. M. M., Hussain, F. F. K., Harrison, A., Bazooyar, B., Zanker, M., & Bureš, V. (2024). A new methodology for reducing carbon emissions

using multi-renewable energy systems and artificial intelligence. *Sustain. Cities Soc., 114*, Article 105721. https://doi.org/10.1016/J.SCS.2024.105721
Alonso, A. P. (2024). Pumped hydro energy storage systems for a sustainable energy planning. *Sustain. Energy Plan. Smart Grids*, 71–89. https://doi.org/10.1016/B978-0-443-14154-6.00014-4
Awad, H., Nassar, Y. F., Hafez, A., Sherbiny, M. K., & Ali, A. F. M. (2022). Optimal design and economic feasibility of rooftop photovoltaic energy system for Assuit University, Egypt. *Ain Shams Eng. J., 13*, Article 101599. https://doi.org/10.1016/J.ASEJ.2021.09.026
Awad, H., Nassar, Y. F., Elzer, R. S., Mangir, I., El-Khozondar, H. J., Khaleel, M., Ahmed, A., Alsharif, A., Salem, M., & Hafez, A. (2023). Energy, economic and environmental feasibility of energy recovery from wastewater treatment plants in mountainous areas: A case study of Gharyan city–Libya. *Acta Innov*.
Beker, B. A., & Kansal, M. L. (2024). *Complexities of the urban drinking water systems in Ethiopia and possible interventions for sustainability, 26*. Netherlands: Springer. ISBN 0123456789.
Bermúdez, J.-R., López-Estrada, F.-R., Besançon, G., Valencia-Palomo, G., & Santos-Ruiz, I. (2022). Predictive control in water distribution systems for leak reduction and pressure management via a pressure reducing valve. *Processes, 10*.
Boroomandnia, A., Rismanchi, B., Wu, W., & Anderson, R. (2024). Optimal design of micro pumped-storage plants in the heart of a city. *Sustain. Cities Soc., 101*, Article 105054. https://doi.org/10.1016/j.scs.2023.105054
Calautit, K., & Johnstone, C. (2023). State-of-the-art review of micro to small-scale wind energy harvesting technologies for building integration. *Energy Convers. Manag. X, 20*, Article 100457. https://doi.org/10.1016/J.ECMX.2023.100457
COST BASE FOR SMALL HYDROPOWER PLANTS IN Georgia < 13 MEGAWATT' Available online: https://www.nve.no/media/11667/cost_base_small_english.pdf (accessed on Jul 1, 2024).
Elghaish, F., Matarneh, S., Hosseini, M. R., Tezel, A., Mahamadu, A. M., & Taghikhah, F. (2024). Predictive digital twin technologies for achieving net zero carbon emissions: A critical review and future research agenda. *Smart Sustain. Built Environ.*. https://doi.org/10.1108/SASBE-03-2024-0096/FULL/PDF. ahead-of-print.
EV Battery Costs - Dropping Faster Than Predicted Even By Tony Seba | Torque News Available online: https://www.torquenews.com/14335/ev-battery-costs-dropping-faster-predicted-even-tony-seba (accessed on Sep 12, 2024).
Fathi Nassar, Y., & Yassin Alsadi, S. (2018). Wind Energy Potential in Gaza Strip-Palestine state. *Sol. Energy Sustain. Dev. J., 7*, 41–57. https://doi.org/10.51646/jsesd.v7i2.40
Fluid Flow Friction Loss - Hazen-Williams Coefficients' Available online: https://www.engineeringtoolbox.com/hazen-williams-coefficients-d_798.html (accessed on Jul 1, 2024).
Fu, G., Jin, Y., Sun, S., Yuan, Z., & Butler, D. (2022). The role of deep learning in urban water management: A critical review. *Water Res, 223*, Article 118973. https://doi.org/10.1016/J.WATRES.2022.118973
Garcia, C., López-Jiménez, P. A., Pérez-Sánchez, M., & Sanchis, R. (2024). Methodology for assessing progress in sustainable development goals indicators in urban water systems. How far are we from the 2030 targets? *Sustain. Cities Soc., 112*, Article 105616. https://doi.org/10.1016/j.scs.2024.105616
Hafez, A. A., Nassar, Y. F., Hammdan, M. I., & Alsadi, S. Y. (2020). Technical and Economic Feasibility of Utility-Scale Solar Energy Conversion Systems in Saudi Arabia. *Iran. J. Sci. Technol. - Trans. Electr. Eng., 44*, 213–225. https://doi.org/10.1007/S40998-019-00233-3/FIGURES/9
Hafez, A. A., Nassar, Y. F., Hammdan, M. I., & Alsadi, S. Y. (2020). Technical and Economic Feasibility of Utility-Scale Solar Energy Conversion Systems in Saudi Arabia. *Iran. J. Sci. Technol. - Trans. Electr. Eng., 44*, 213–225. https://doi.org/10.1007/S40998-019-00233-3/FIGURES/9
Hille, E. (2023). Europe's energy crisis: Are geopolitical risks in source countries of fossil fuels accelerating the transition to renewable energy? *Energy Econ., 127*, Article 107061. https://doi.org/10.1016/J.ENECO.2023.107061
Jafari, S. M., Nikoo, M. R., Bozorg-Haddad, O., Alamdari, N., Farmani, R., & Gandomi, A. H. (2023). A robust clustering-based multi-objective model for optimal instruction of pipes replacement in urban WDN based on machine learning approaches. *Urban Water J, 20*, 689–706. https://doi.org/10.1080/1573062X.2023.2209063
Kakoulaki, G., Taylor, N., Szabo, S., Kenny, R., Chatzipanagi, A., & Jäger-Waldau, A. (2024). Communication on the potential of applied PV in the European Union: Rooftops, reservoirs, roads (R3). *EPJ Photovoltaics, 15*(2). https://doi.org/10.1051/EPJPV/2023035
Kamyab, H., Khademi, T., Chelliapan, S., SaberiKamarposhti, M., Rezania, S., Yusuf, M., Farajnezhad, M., Abbas, M., Hun Jeon, B., & Ahn, Y. (2023). The latest innovative avenues for the utilization of artificial Intelligence and big data analytics in water resource management. *Results Eng, 20*, Article 101566. https://doi.org/10.1016/j.rineng.2023.101566
Karlilar Pata, S., & Balcilar, M. (2024). Decarbonizing energy: Evaluating fossil fuel displacement by renewables in OECD countries. *Environ. Sci. Pollut. Res., 31*, 31304–31313. https://doi.org/10.1007/S11356-024-33324-8/TABLES/5
Kavya, M., Mathew, A., Shekar, P. R., & P, S (2023). Short term water demand forecast modelling using artificial intelligence for smart water management. *Sustain. Cities Soc., 95*, Article 104610. https://doi.org/10.1016/j.scs.2023.104610
Khalid, M. (2024). Smart grids and renewable energy systems: Perspectives and grid integration challenges. *Energy Strateg. Rev., 51*, Article 101299. https://doi.org/10.1016/J.ESR.2024.101299
Khan, T., Yu, M., & Waseem, M. (2022). Review on recent optimization strategies for hybrid renewable energy system with hydrogen technologies: State of the art, trends and future directions. *Int. J. Hydrogen Energy, 47*, 25155–25201. https://doi.org/10.1016/J.IJHYDENE.2022.05.263
Magini, R., Moretti, M., Boniforti, M. A., & Guercio, R. (2023). A Machine-Learning Approach for Monitoring Water Distribution Networks (WDNs). *Sustainability, 15*.
Mercedes Garcia, A. V., Sánchez-Romero, F. J., López-Jiménez, P. A., & Pérez-Sánchez, M (2022). A new optimization approach for the use of hybrid renewable systems in the search of the zero net energy consumption in water irrigation systems. *Renew. Energy, 195*, 853–871. https://doi.org/10.1016/J.RENENE.2022.06.060
Moasheri, R., Ghazizadeh, M. J., & Tashayoei, M. (2021). Leakage detection in water networks by a calibration method. *Flow Measurement and Instrumentation*. Tehran, Iran: Elsevier Ltd, Article 101995. Vol. 80.
Mokhtara, C., Negrou, B., Settou, N., Bouferrouk, A., & Yao, Y. (2021). Optimal design of grid-connected rooftop PV systems: An overview and a new approach with application to educational buildings in arid climates. *Sustain. Energy Technol. Assessments, 47*, Article 101468. https://doi.org/10.1016/J.SETA.2021.101468
Morosini, A. F., Haghshenas, S. S., Haghshenas, S. S., Choi, D. Y., & Geem, Z. W. (2021). Sensitivity analysis for performance evaluation of a real water distribution system by a pressure driven analysis approach and artificial intelligence method. *Water (Switzerland), 13*. https://doi.org/10.3390/w13081116
Nassar, Y. F., & Salem, A. A. (2007). The reliability of the photovoltaic utilization in southern cities of Libya. *Desalination, 209*, 86–90. https://doi.org/10.1016/J.DESAL.2007.04.013
Nassar, Y. F., Abdunnabi, M. J., Sbeta, M. N., Hafez, A. A., Amer, K. A., Ahmed, A. Y., & Belgasim, B. (2021). Dynamic analysis and sizing optimization of a pumped hydroelectric storage-integrated hybrid PV/Wind system: A case study. *Energy Convers. Manag., 229*, Article 113744. https://doi.org/10.1016/j.enconman.2020.113744
Nassar, Y. F., Alsadi, S. Y., El-Khozondar, H. J., Ismail, M. S., Al-Maghalseh, M., Khatib, T., Sa'ed, J. A., Mushtaha, M. H., & Djerafi, T. (2022). Design of an isolated renewable hybrid energy system: a case study. *Mater. Renew. Sustain. Energy, 11*, 225–240. https://doi.org/10.1007/s40243-022-00216-1
Nassar, Y., Mangir, I., Hafez, A., El-Khozondar, H., Salem, M., & Awad, H. (2023). Feasibility of innovative topography-based hybrid renewable electrical power system: A case study. *Clean. Eng. Technol., 14*, Article 100650. https://doi.org/10.1016/J.CLET.2023.100650
Nassar, Y. F., El-Khozondar, H. J., El-Osta, W., Mohammed, S., Elnaggar, M., Khaleel, M., & Ahmed, A. (2024). Alsharif, A. Carbon footprint and energy life cycle assessment of wind energy industry in Libya. *Energy Convers. Manag., 300*, Article 117846. https://doi.org/10.1016/j.enconman.2023.117846
Nassar, Y. F., El-Khozondar, H. J., Elnaggar, M., El-batta, F. F., El-Khozondar, R. J., & Alsadi, S. Y. (2024). Renewable energy potential in the State of Palestine: Proposals for sustainability. *Renew. Energy Focus, 49*, Article 100576. https://doi.org/10.1016/J.REF.2024.100576
Nassar, Y. F., El-Khozondar, H. J., Alatrash, A. A., Ahmed, B. A., Elzer, R. S., Ahmed, A. A., Imbayah, I. I., Alsharif, A. H., & Khaleel, M. M. (2024). Assessing the Viability of Solar and Wind Energy Technologies in Semi-Arid and Arid Regions: A Case Study of Libya's Climatic Conditions. *Appl. Sol. Energy (English Transl. Geliotekhnika), 60*, 149–170. https://doi.org/10.3103/S0003701x24600218/FIGURES/8
Ogayar, B., & Vidal, P. G. (2009). Cost determination of the electro-mechanical equipment of a small hydro-power plant. *Renew. Energy, 34*, 6–13. https://doi.org/10.1016/J.RENENE.2008.04.039
Onshore Wind Turbine SG 2.1-114 | Siemens Gamesa Available online: https://www.siemensgamesa.com/en-int/products-and-services/onshore/wind-turbine-sg-2-1-114 (accessed on Jul 1, 2024).
Pérez-Collazo, C., Greaves, D., & Iglesias, G. (2015). A review of combined wave and offshore wind energy. *Renew. Sustain. Energy Rev., 42*, 141–153. https://doi.org/10.1016/J.RSER.2014.09.032
PARTNER SECTION TEMPERATURE CHARACTERISTICS Available online: www.csisolar.com (accessed on Jul 1, 2024).
Positioning of Danish offshore wind farms until 2030 – using Levelized Cost of Energy (LCoE) — Welcome to DTU Research Database Available online: https://orbit.dtu.dk/en/projects/positioning-of-danish-offshore-wind-farms-until-2030-using-leveli (accessed on Sep 12, 2024).
Ramos, H.M.; Almeida, A. SMALL HYDRO AS ONE OF THE OLDEST RENEWABLE ENERGY SOURCES Available online: https://www.researchgate.net/profile/Helena_Ramos3/publication/237532453_SMALL_HYDRO_AS_ONE_OF_THE_OLDEST_RENEWABLE_ENERGY_SOURCES/links/00b49539d55ea83c01000000.pdf (accessed on Feb 9, 2016).
Ramos, H. M., Vargas, B., & Saldanha, J. R. (2022). New Integrated Energy Solution Idealization: Hybrid for Renewable Energy Network (Hy4REN). *Energies, 15*.
Ramos, H. M., Sintong, J. E., & Kuriqi, A. (2024). Optimal integration of hybrid pumped storage hydropower toward energy transition. *Renew. Energy, 221*, Article 119732. https://doi.org/10.1016/J.RENENE.2023.119732
Ramos, H. *Guidelines for Design of Small hydropower plants*; Ramos, H., Ed.; 2000.
Ren, Y., Sun, K., Zhang, K., Han, Y., Zhang, H., Wang, M., Jing, X., Mo, J., Zou, W., & Xing, X. (2024). Optimization of the capacity configuration of an abandoned mine pumped storage/wind/photovoltaic integrated system. *Appl. Energy, 374*, Article 124089. https://doi.org/10.1016/j.apenergy.2024.124089
Saheb, D., Koussa, M., & Hadji, S. (2014). Technical and economical study of a stand-alone wind energy system for remote rural area electrification in Algeria. *Renew. Energy Power Qual. J., 1*, 638–643. https://doi.org/10.24084/repqj12.439
Satymov, R., Bogdanov, D., & Breyer, C. (2022). Global-local analysis of cost-optimal onshore wind turbine configurations considering wind classes and hub heights. *Energy, 256*, Article 124629. https://doi.org/10.1016/J.ENERGY.2022.124629
Sayed, E. T., Olabi, A. G., Elsaid, K., Al Radi, M., Semeraro, C., Doranehgard, M. H., Eltayeb, M. E., & Abdelkareem, M. A. (2023). Application of artificial intelligence techniques for modeling, optimizing, and controlling desalination systems powered

by renewable energy resources. *J. Clean. Prod., 413*, Article 137486. https://doi.org/10.1016/J.JCLEPRO.2023.137486

Schmitt, R. J. P., & Rosa, L. (2024). Dams for hydropower and irrigation: Trends, challenges, and alternatives. *Renew. Sustain. Energy Rev., 199*, Article 114439. https://doi.org/10.1016/j.rser.2024.114439

Seme, S., Sredenšek, K., Praunseis, Z., Štumberger, B., & Hadžiselimović, M. (2018). Optimal price of electricity of solar power plants and small hydro power plants – Technical and economical part of investments. *Energy, 157*, 87–95. https://doi.org/10.1016/J.ENERGY.2018.05.121

Suresh, A., Kishorekumar, R., Kumar, M. S., & Elaiyaraja, K. (2022). Assessing transmission excellence and flow detection based on Machine Learning. *Opt. Quantum Electron., 54*, 1–12. https://doi.org/10.1007/S11082-022-03867-6/FIGURES/5

Vartiainen, E., Masson, G., Breyer, C., Moser, D., & Román Medina, E. (2020). Impact of weighted average cost of capital, capital expenditure, and other parameters on future utility-scale PV levelised cost of electricity. *Prog. Photovoltaics Res. Appl., 28*, 439–453. https://doi.org/10.1002/pip.3189

Wang, S., Taha, A. F., & Abokifa, A. A. (2021). How Effective is Model Predictive Control in Real-Time Water Quality Regulation? State-Space Modeling and Scalable Control. *Water Resour. Res., 57*, Article e2020WR027771. https://doi.org/10.1029/2020WR027771

Wind Turbine Spacing: How Far Apart Should They Be? - Energy Follower' Available online: https://energyfollower.com/wind-turbine-spacing/(accessed on Jul 1, 2024).

Wu, Z. Y., Chew, A., Meng, X., Cai, J., Pok, J., Kalfarisi, R., Lai, K. C., Hew, S. F., & Wong, J. J. (2023). High Fidelity Digital Twin-Based Anomaly Detection and Localization for Smart Water Grid Operation Management. *Sustain. Cities Soc., 91*, Article 104446. https://doi.org/10.1016/J.SCS.2023.104446

Xiang, X., Li, Q., Khan, S., & Khalaf, O. I. (2021). Urban water resource management for sustainable environment planning using artificial intelligence techniques. *Environ. Impact Assess. Rev., 86*, Article 106515. https://doi.org/10.1016/J.EIAR.2020.106515

Xiang, P., Jiang, K., Wang, J., He, C., Chen, S., & Jiang, W. (2024). Evaluation of LCOH of conventional technology, energy storage coupled solar PV electrolysis, and HTGR in China. *Appl. Energy, 353*, Article 122086. https://doi.org/10.1016/j.apenergy.2023.122086